

Fractured Meshes

M. Averseng and X. Claeys and R. Hiptmair

Research Report No. 2022-14
April 2022

Seminar für Angewandte Mathematik
Eidgenössische Technische Hochschule
CH-8092 Zürich
Switzerland

Fractured meshes

Martin Averseng, Xavier Claeys, Ralf Hiptmair

April 14, 2022

Abstract

This work introduces a concept of “generalized meshes”, similar to simplicial meshes, but allowing for overlapping elements, and with adjacency relations that are defined independently from the number of shared vertices. This additional flexibility allows for the representation of complex geometries such as fractured meshes and two sided complex surfaces. The generalized mesh is then a convenient object to accompany a numerical method, as its so-called “generalized subfacets” play naturally the role of degrees of freedom for finite/boundary element methods. Our emphasis is on precise definitions and proofs, as well as numerical implementation especially for the boundary element applications.

Keywords: Fractures, Meshes, Boundary Elements, Finite elements.

Introduction

For an n -dimensional domain $\Omega \subset \mathbb{R}^n$, a fracture may be modeled by an embedded $(n - 1)$ -dimensional structure. There are two points of view.

- (i) In the first one, the physical equations are posed in the domain Ω surrounding the fracture, with boundary conditions on $\partial\Omega$ and Γ . A key example is the so-called mixed-dimensional modeling of flow in fractured porous media. References on this topic include [1, Section 5], [11, Section 3.5], [2, 4, 12, 24, 28] but the list is far from being exhaustive.
- (ii) In the second one, the physical equations are formulated directly and only on the surface of Γ . This is the approach followed for example in wave scattering problems, where the obstacle Γ is a complex screen embedded in the space \mathbb{R}^3 . A lot of attention has been devoted to the analysis and numerical resolution of this type of problem in recent years. References include [9, 15, 16, 18, 19, 23].

We adapt the notion of fractures to triangulated domains and treat both perspectives in a unified way. We introduce a mathematical structure, called *generalized mesh*, that enlarges the class of usual regular simplicial meshes to allow for some more flexibility, while retaining good properties with respect to the action of the boundary operator. In generalized meshes, simplices are allowed to overlap arbitrarily, and their mutual adjacency is supplied as part of the definition of the mesh, independently from the number of shared vertices. Through generalized meshes, perspectives (i) and (ii) are connected via a *boundary* operator that maps an n -dimensional to an $(n - 1)$ -dimensional generalized mesh.

In some parts of this work, readers with a fracture mechanics background (point of view (i)) will find familiar concepts, that are a standard part of modern codes. For instance, the automatic splitting of mesh vertices into independent copies at a fracture intersection – here formalized through the concept of *generalized vertices* – is well established (see e.g. [24, Fig. 8]), and can be considered as “common-practice” knowledge.

Nevertheless, the mathematical formalization and rigorous treatment of those fairly well-spread ideas bears fruits, especially in the second perspective. For instance, the automatic splitting of vertices located on the fracture is also possible even when the surrounding mesh is not available (see Section 4.4). This removes the need for manual intervention in the mesh construction for the boundary element multi-screen solver. It also unlocks useful results for the analysis such as Theorem 2.

The paper is organized as follows: in Section 1, we review some combinatorial geometry background. We then define generalized meshes in Section 2, and their boundary in Section 3, and we show that it generalizes the usual concept of boundary. In Section 4, we focus on factured meshes and their boundary. We present an algorithm to reconstruct the boundary without relying on a mesh of the surrounding volume. In Section 5, we define spaces of Whitney forms and study the surjectivity of a trace operator relating those spaces for a generalized mesh and its boundary. Finally, some numerical experiments are presented in Section 6.

For the reader’s convenience a list of frequently used notation is provided in the end of the article.

1 Preliminaries

1.1 Simplices and orientation

In this work, an n -simplex S is a subset of cardinality $(n + 1)$ of some vertex set \mathcal{V} (for example, but not necessarily, $\mathcal{V} = \mathbb{R}^3$). The elements of S are called its *vertices*. Let $\sigma_d(S)$ denote the set of $(d + 1)$ -subsets of S , also called d -subsimplices of S . The $(n - 1)$ -subsimplices are called facets and we write $\mathcal{F}(S) := \sigma_{n-1}(S)$. The set of all subsimplices of S , including S , is denoted by $\sigma(S)$. An n -simplex is called a vertex, an edge, a triangle and a tetrahedron for $n = 0, 1, 2$ and 3 .

When the vertices of an n -simplex S are points in \mathbb{R}^m with $n \leq m$, we systematically assume that they are affinely independent, and we denote by $|S|$ the closed convex hull of S :¹

$$|S| = \text{Hull}(\{V_1, \dots, V_{n+1}\}) := \left\{ \sum_{i=1}^{n+1} \lambda_i V_i \mid \forall i \in \{1 \dots, n+1\}, \lambda_i \geq 0, \sum_{i=1}^{n+1} \lambda_i = 1 \right\}. \quad (1)$$

For $n \geq 1$, an *orientation* of a simplex S is an ordering V_1, \dots, V_{n+1} of its vertices, with the rule that two orderings define the same orientation if they differ by an even permutation. If $n = 0$, i.e. when S is a vertex, an orientation of S is simply an element of $\{+, -\}$.

An *oriented simplex* $[S]$ is a simplex S together with a choice of orientation. As in [26, Chap. 5], we denote by $[V_1, \dots, V_{n+1}]$ the simplex $\{V_1, \dots, V_{n+1}\}$ oriented by the order V_1, \dots, V_{n+1} . Given an oriented simplex $[S]$, we denote by and by $-[S]$ the same simplex with the opposite orientation. Hence for example

$$[A, B, C, D] = -[A, C, B, D] = [C, A, B, D].$$

¹In most reference, a simplex is defined as the convex hull of its vertices, but the definition that we adopt here, (i.e. a simplex is defined as a finite set of vertices) is more convenient for our needs.

When $n \geq 2$, an oriented n -simplex $[S] = [V_1, \dots, V_{n+1}]$ induces an orientation on its facets: for the facet $F_i = \{V_1, \dots, \widehat{V}_i, \dots, V_{n+1}\}$, where the hat denotes an omission, the induced orientation is defined by

$$[F_i]_{|[S]} := (-1)^{i+1} [V_1, \dots, \widehat{V}_i, \dots, V_{n+1}]. \quad (2)$$

For $n = 1$, given an oriented edge $E = [V_1, V_2]$, we take the convention

$$[V_1]_{|[E]} := [V_1, -], \quad [V_2]_{|[E]} := [V_2, +].$$

Two oriented n -simplices $[S_1]$ and $[S_2]$, with $n \geq 1$, sharing a facet F , are *consistently oriented* if

$$[F]_{|[S_1]} = -[F]_{|[S_2]} \quad (3)$$

i.e. they induce **opposite** orientations on their common facet. One has the following elementary result:

Lemma 1. *If $[K]$ is an oriented n -simplex with $n \geq 2$, and F and F' are two distinct facets of K , then $[F]_{|[K]}$ and $[F']_{|[K]}$ are consistently oriented.*

If $\mathcal{V} \subset \mathbb{R}^n$, the n -simplices have a *natural orientation*: $[V_1, \dots, V_{n+1}]$ is naturally oriented if

$$\det [V_2 - V_1, \dots, V_{n+1} - V_1] > 0.$$

Let us mention the following result (see e.g. the proof of [26, Prop. 5.16])

Lemma 2. *Let $[K]$ and $[K']$ be two naturally oriented n -simplices in \mathbb{R}^n that share a facet, but have disjoint interiors. Then $[K]$ and $[K']$ are consistently oriented.*

Choosing an orientation of a triangle T in \mathbb{R}^3 is equivalent to deciding on a unit normal vector \mathbf{n} on T : the orientation $[A, B, C]$ corresponds to the vector

$$\mathbf{n} = \frac{\overrightarrow{AB} \times \overrightarrow{AC}}{\|\overrightarrow{AB} \times \overrightarrow{AC}\|}. \quad (4)$$

1.2 Abstract triangulations

An n -dimensional *abstract triangulation* (or simply triangulation) \mathcal{M} is a finite set of n -simplices that we call the *elements* of \mathcal{M} . The d -*subsimplices* of \mathcal{M} are defined as the d -subsimplices of its elements:

$$\sigma_d(\mathcal{M}) := \bigcup_{K \in \mathcal{M}} \sigma_d(K), \quad \mathcal{F}(\mathcal{M}) := \sigma_{n-1}(\mathcal{M}), \quad \sigma(\mathcal{M}) := \bigcup_{d \leq n} \sigma_d(\mathcal{M}). \quad (5)$$

With those definitions, $\sigma(\mathcal{M})$ is a *pure* abstract simplicial complex, see e.g. [29, Chap. 7].

In an abstract triangulation \mathcal{M} , we say that $S \in \sigma_d(\mathcal{M})$ and $S' \in \sigma_{d'}(\mathcal{M})$ are *incident* if

$$|d - d'| = 1 \text{ and } S \subset S' \text{ or } S' \subset S.$$

Two d -subsimplices S and S' are *adjacent* if they are incident to a common $(d-1)$ -subsimplex, in which case we write $S \overset{\mathcal{M}}{\longleftrightarrow} S'$. An abstract triangulation \mathcal{M} is *branching* if at least one facet of \mathcal{M} is incident to more than two elements of \mathcal{M} , and *non-branching* otherwise.

Given a subsimplex $S \in \sigma(\mathcal{M})$, the *star* and the *link* (see e.g. [14, p.3]) of S are the abstract triangulations defined by

$$\text{st}(S, \mathcal{M}) := \{K \in \mathcal{M} \mid S \subset K\}, \quad (6)$$

$$\text{lk}(S, \mathcal{M}) := \{S' \in \sigma(\mathcal{M}) \mid S \cap S' = \emptyset, (S \cup S') \in \mathcal{M}\}. \quad (7)$$

For $n \geq 1$, the *boundary* $\partial\mathcal{M}$ of an n -dimensional triangulation \mathcal{M} is the $(n - 1)$ -dimensional triangulation defined by

$$\partial\mathcal{M} := \{F \in \mathcal{F}(\mathcal{M}) \mid F \text{ is incident to exactly one element of } \mathcal{M}\}. \quad (8)$$

When $n = 0$, we define $\partial\mathcal{M}$ as the empty set. Hence for example if

$$\mathcal{M} = \{\{A, B, C\}, \{A, B, D\}, \{A, C, D\}, \{B, C, D\}, \{C, D, E\}\}, \quad \mathcal{V} = \{A, B, C, D, E\}$$

then $\partial\mathcal{M} = \{\{C, E\}, \{D, E\}\}$, $\partial\partial\mathcal{M} = \{\{C\}, \{D\}\}$ and $\partial\partial\partial\mathcal{M} = \emptyset$. One can check that if \mathcal{M} is non-branching, then $\partial\partial\mathcal{M} = \emptyset$. The boundary of a non-branching triangulation can be branching, for example

$$\mathcal{M} = \{\{A, B, C\}, \{C, D, E\}\} \quad (9)$$

is non-branching, while its boundary is branching.

An *orientation* of a triangulation \mathcal{M} is a choice of an orientation of each of its simplices. An *oriented triangulation* is a triangulation equipped with an orientation. If \mathcal{M} is oriented, the oriented simplex corresponding to the element $K \in \mathcal{M}$ is denoted by $[K]_{\mathcal{M}}$.

The orientation of \mathcal{M} is called *compatible* if for any two adjacent elements K and K' , $[K]_{\mathcal{M}}$ and $[K']_{\mathcal{M}}$ are consistently oriented. An abstract triangulation which admits a compatible orientation is called *orientable*. Obviously, an orientable triangulation must be non-branching. Hence, the example (9) above also shows that an orientable triangulation can have a non-orientable boundary.

1.3 Simplicial meshes

An n -dimensional abstract triangulation \mathcal{M} is called a *simplicial mesh* (or simply mesh) if the associated vertex set \mathcal{V} is a subset of \mathbb{R}^m , with $n \leq m$ and if

$$\forall(K, K') \in \mathcal{M} \times \mathcal{M}, \quad |K| \cap |K'| = |K \cap K'|. \quad (10)$$

We write

$$|\mathcal{M}| := \bigcup_{K \in \mathcal{M}} |K|, \quad (11)$$

and say that \mathcal{M} is *regular* if $|\mathcal{M}|$ is an n -manifold with or without boundary, meaning that each point $x \in |\mathcal{M}|$ has a neighborhood in $|\mathcal{M}|$ that is homeomorphic to either \mathbb{R}^n or $\mathbb{R}_+^n := \mathbb{R}^{n-1} \times \mathbb{R}^+$.

It is a well-known result of piecewise linear topology (see e.g. [30, Ex. 2.21(i)]) that an n -dimensional mesh is regular if and only if the link of any vertex is piecewise linearly homeomorphic to either $[0, 1]^{n-1}$ or $\partial([0, 1]^n)$.² A simplicial complex satisfying this property is called a triangulation in [13], and a combinatorial n -manifold in [14]. An example of a non-regular mesh is given by Figure 1, while Figure 2 shows the link and the star of a vertex in a regular mesh.

²The definition of a piecewise linear homeomorphism can be found e.g. in [14, p.3].

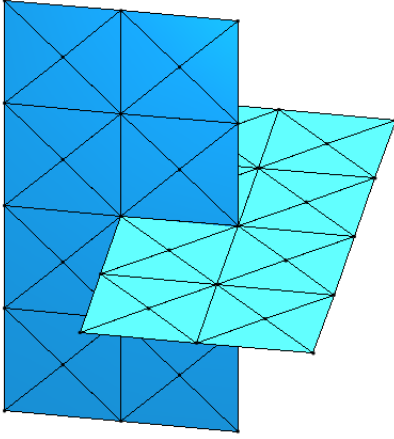


Figure 1: Example of a non-regular triangular mesh. This and some other examples in this paper are constructed using Gmsh [22].

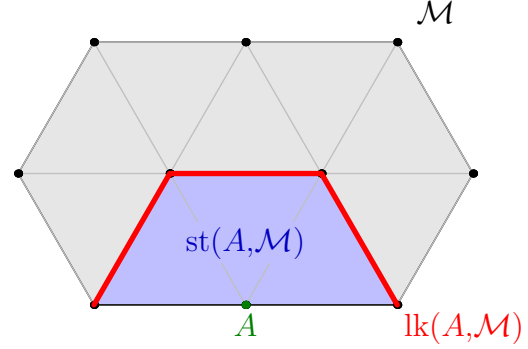


Figure 2: An example of regular triangular mesh. The link (resp. the star) of the vertex A , represented in red, (resp. in blue) is homeomorphic to $[0, 1]$ (resp. $[0, 1]^2$).

Every facet of a regular mesh is incident to at most two elements (see e.g. [13, Lemma 11.1.2]). Hence, when $n = 3$, this notion of regular mesh also corresponds to that of Ciarlet [17, Chap. 2], which is well-established in finite element literature. The previous observation also implies that regular meshes are a particular case of non-branching triangulations. Moreover, when \mathcal{M} is regular, then so is its boundary $\partial\mathcal{M}$, and $|\partial\mathcal{M}|$ is the manifold boundary of $|\mathcal{M}|$ (cf. [14, p. 4]).

We also record the following classical property of regular meshes for later use:

Lemma 3. *If \mathcal{M} is a regular mesh and $S \in \sigma(\mathcal{M})$, then the star of S is face-connected, in the sense that given two elements K and K' in $\text{st}(S, \mathcal{M})$, there are elements K_1, \dots, K_Q of $\text{st}(S, \mathcal{M})$ such that*

- (i) $K_1 = K$
- (ii) $K_Q = K'$
- (iii) $\forall i \in \{1, \dots, Q-1\}, K_i \xleftrightarrow[\mathcal{M}]{} K_{i+1}$.

Proof. Following the comment below Theorem 2.2 in [14], the mesh $\text{st}(S, \mathcal{M})$ is piecewise linearly homeomorphic to $[0, 1]^n$. In particular, it is a connected regular mesh, so the result follows from [13, Lemma 11.1.3]. \square

1.4 Data structures

We provide a Matlab implementation as supplementary material [6], in which simplicial meshes over $\mathcal{V} \subset \mathbb{R}^3$ are manipulated via the toolbox `openMsh` from [3]. The mesh class is defined as follows

```

classdef msh
properties
    vtx;    % Nvtx x 3 array of reals coordinates
    elt;    % Nelt x (n+1) array with entries in {1,...,Nvtx}
end

```

The points of \mathcal{V} are stored in the array `vtx`. Each line of this array corresponds to a vertex $V \in \mathcal{V}$, the three column giving the x, y and z coordinates. The lines of the array `elt` are mutually distinct and encode the simplices of \mathcal{M} , referring to the vertices by their index in `vtx`. This is essentially the same data structure as the one used in the standard meshing tool Gmsh [22]. Let us mention that alternative choices of data structure to represent more general simplicial complexes are also common, see e.g. [20] for a review.

2 Generalized meshes

We now introduce a more flexible type of mesh, where elements can overlap arbitrarily, and where adjacency is not defined by the number of shared vertices between elements, but directly supplied as part of the definition.

2.1 Definitions

Definition 1 (Generalized mesh). For $n \geq 0$, an n -dimensional *generalized mesh* \mathcal{M}^* is a quadruple $(\mathcal{V}_{\mathcal{M}^*}, \mathbf{K}_{\mathcal{M}^*}, \mathcal{K}_{\mathcal{M}^*}, \mathcal{G}_{\mathcal{M}^*})$ where

- $\mathcal{V}_{\mathcal{M}^*}$ is a set called the *vertex set* of \mathcal{M}^* .
- $\mathbf{K}_{\mathcal{M}^*}$ is a finite set. Its elements are called *elements* of \mathcal{M}^* , and we write $\mathbf{k} \in \mathcal{M}^*$ as short for $\mathbf{k} \in \mathbf{K}_{\mathcal{M}^*}$.
- $\mathcal{K}_{\mathcal{M}^*}$ is a *realization function*, mapping each element of $\mathbf{k} \in \mathcal{M}^*$ to a simplex $\mathcal{K}_{\mathcal{M}^*}(\mathbf{k})$ with vertices in $\mathcal{V}_{\mathcal{M}^*}$. The simplex $\mathcal{K}_{\mathcal{M}^*}(\mathbf{k})$ is called *the simplex attached to \mathbf{k}* . If $\mathcal{V}_{\mathcal{M}^*} \subset \mathbb{R}^m$ for some $m \geq n$, then the simplices attached to the elements of \mathcal{M}^* are assumed to be non-degenerate. The realization function need not be injective: the same simplex may be attached to several distinct elements.
- $\mathcal{G}_{\mathcal{M}^*}$ is a graph between the split facets of \mathcal{M}^* , by which we mean the pairs of the form

$$(F, \mathbf{k}), \text{ with } \mathbf{k} \in \mathcal{M}^* \text{ and } F \text{ a facet of } K = \mathcal{K}_{\mathcal{M}^*}(\mathbf{k}). \quad (12)$$

We write $\mathbb{F}(\mathcal{M}^*)$ for the set of split facets. The graph $\mathcal{G}_{\mathcal{M}^*}$ is called *the adjacency graph* of \mathcal{M}^* , and is assumed to satisfy the following axioms:

- (i) the nodes of $\mathcal{G}_{\mathcal{M}^*}$ have degree 0 or 1, and

(ii) if two split facets (F, \mathbf{k}) and (F', \mathbf{k}') are connected by an edge in $\mathcal{G}_{\mathcal{M}^*}$, then

$$F = F' \text{ and } \mathbf{k} \neq \mathbf{k}'.$$

When the split facets (F, \mathbf{k}) and (F', \mathbf{k}') are connected by an edge in $\mathcal{G}_{\mathcal{M}^*}$, we write

$$\mathbf{k} \xleftrightarrow[\mathcal{M}^*]{F} \mathbf{k}', \quad (13)$$

and say that \mathbf{k} and \mathbf{k}' are *adjacent through F* . If $\mathbf{k} \xleftrightarrow[\mathcal{M}^*]{F} \mathbf{k}'$ and $S \in \sigma(F)$, then we also say that \mathbf{k} and \mathbf{k}' are adjacent through S and extend the notation $\mathbf{k} \xleftrightarrow[\mathcal{M}^*]{S} \mathbf{k}'$ to this case.

For each split facet $(F, \mathbf{k}) \in \mathbb{F}(\mathcal{M}^*)$, by requirement (i), there is at most one element \mathbf{k}' such that $\mathbf{k} \xleftrightarrow[\mathcal{M}^*]{F} \mathbf{k}'$. If such an element exist, it is called *the neighbor of \mathbf{k} through F* . Otherwise, we write $\mathbf{k} \xleftrightarrow[\mathcal{M}^*]{F} \perp$. Hence, for each element $\mathbf{k} \in \mathcal{M}^*$, we can define a *neighbor function*

$$\mathcal{N}_{\mathcal{M}^*}(\mathbf{k}, \cdot) : \mathcal{F}(K) \rightarrow \mathbf{K}_{\mathcal{M}^*}$$

mapping each facet F of the simplex $K = \mathcal{K}_{\mathcal{M}^*}(\mathbf{k})$ to the neighbor of \mathbf{k} through F :

$$\forall F \in \mathcal{F}(K), \quad \mathcal{N}_{\mathcal{M}^*}(\mathbf{k}, F) := \begin{cases} \mathbf{k}' & \text{if } \mathbf{k} \xleftrightarrow[\mathcal{M}^*]{F} \mathbf{k}', \\ \perp & \text{if } \mathbf{k} \xleftrightarrow[\mathcal{M}^*]{F} \perp. \end{cases} \quad (14)$$

When the generalized mesh under consideration is sufficiently clear from the context, we drop the subscript \mathcal{M}^* , i.e. write $\mathcal{V}, \mathbf{K}, \mathcal{K}, \mathcal{G}, \xleftrightarrow{F}$, instead of $\mathcal{V}_{\mathcal{M}^*}, \mathbf{K}_{\mathcal{M}^*}, \mathcal{K}_{\mathcal{M}^*}, \mathcal{G}_{\mathcal{M}^*}, \xleftrightarrow[\mathcal{M}^*]{F}$, and so on.

Definition 2 (Subsimplices of a generalized mesh). The subsimplices and facets of an element $\mathbf{k} \in \mathcal{M}^*$ are defined by

$$\sigma_d(\mathbf{k}) := \sigma_d(K), \quad \sigma(\mathbf{k}) := \sigma(K), \quad \mathcal{F}(\mathbf{k}) := \mathcal{F}(K),$$

where K is the simplex attached to \mathbf{k} . If K is a non-degenerate simplex of \mathbb{R}^m , we also write $|\mathbf{k}| := |K|$. Similarly, the subsimplices and facets of a generalized mesh \mathcal{M}^* are

$$\sigma_d(\mathcal{M}^*) := \bigcup_{\mathbf{k} \in \mathbf{K}_{\mathcal{M}^*}} \sigma_d(\mathbf{k}), \quad \sigma(\mathcal{M}^*) := \bigcup_{0 \leq d \leq n} \sigma_d(\mathcal{M}^*), \quad \mathcal{F}(\mathcal{M}^*) := \sigma_{n-1}(\mathcal{M}^*). \quad (15)$$

Definition 3 (Relabeling of generalized meshes). The generalized mesh \mathcal{M}_2^* is a *relabeling* of the generalized mesh \mathcal{M}_1^* if

- there is a bijection $\varphi : \mathbf{K}_{\mathcal{M}_1^*} \rightarrow \mathbf{K}_{\mathcal{M}_2^*}$,

- the realizations functions $\mathcal{K}_{\mathcal{M}_1^*}$ and $\mathcal{K}_{\mathcal{M}_2^*}$ satisfy

$$\mathcal{K}_{\mathcal{M}_1^*} = \mathcal{K}_{\mathcal{M}_2^*} \circ \varphi,$$

- there holds

$$\mathbf{k} \xleftrightarrow[\mathcal{M}_1^*]{F} \mathbf{k}' \iff \varphi(\mathbf{k}) \xleftrightarrow[\mathcal{M}_2^*]{F} \varphi(\mathbf{k}').$$

Every non-branching simplicial mesh can also be regarded as a generalized mesh, in the following sense:

Definition 4 (Generalized mesh representing a non-branching mesh). The generalized mesh \mathcal{M}^* representing the non-branching mesh \mathcal{M} is defined as follows:

- the vertex set is the same as that of \mathcal{M} , i.e. $\mathcal{V}_{\mathcal{M}^*} := \sigma_0(\mathcal{M})$,
- the elements of \mathcal{M}^* are the elements of \mathcal{M} , i.e. $\mathbf{K}_{\mathcal{M}^*} := \mathcal{M}$,
- the realization of \mathcal{M}^* is the identity map, i.e. $\mathcal{K}_{\mathcal{M}^*}(K) = K$, $\forall K \in \mathcal{M}$,
- the adjacency graph is defined by

$$K \xleftrightarrow[\mathcal{M}^*]{F} K' \iff K \xleftrightarrow[\mathcal{M}]{F} K' \iff F = K \cap K'.$$

It is necessary for \mathcal{M} to be non-branching for the adjacency graph in the definition above to satisfy the requirement (i) of Definition 1.

Finally, one can define a notion of orientability for generalized meshes as for simplicial meshes:

Definition 5 (Orientable generalized mesh). An *oriented* generalized mesh is a generalized mesh endowed with an *orientation*, i.e. a choice of orientation for each of its elements. For an element $\mathbf{k} \in \mathcal{M}^*$, an orientation of \mathbf{k} is an orientation of its realization $\mathcal{K}_{\mathcal{M}^*}(\mathbf{k})$. We denote the corresponding oriented simplex by $[\mathbf{k}]_{\mathcal{M}^*}$.

The orientation of \mathcal{M}^* is called *compatible* if, for two adjacent elements \mathbf{k} and \mathbf{k}' , the simplices $[\mathbf{k}]_{\mathcal{M}^*}$ and $[\mathbf{k}']_{\mathcal{M}^*}$ are consistently oriented. A generalized mesh that admits a compatible orientation is called *orientable*.

2.2 Examples

Example 1 (Domain with a crack). Let \mathcal{M}_1^* (represented in Figure 3) be the generalized triangular mesh defined by

$$\mathcal{V} = \{A, \dots, J\}, \quad \mathbf{K} = \{1, \dots, 10\},$$

with the realization

$$\mathcal{K}(1) = ABC, \quad \mathcal{K}(2) = BCD, \quad \mathcal{K}(3) = BDE, \quad \mathcal{K}(4) = BEF, \quad \mathcal{K}(5) = BFG$$

$$\mathcal{K}(6) = ABG, \quad \mathcal{K}(7) = AGH, \quad \mathcal{K}(8) = AHI, \quad \mathcal{K}(9) = AIJ, \quad \mathcal{K}(10) = ACJ.$$

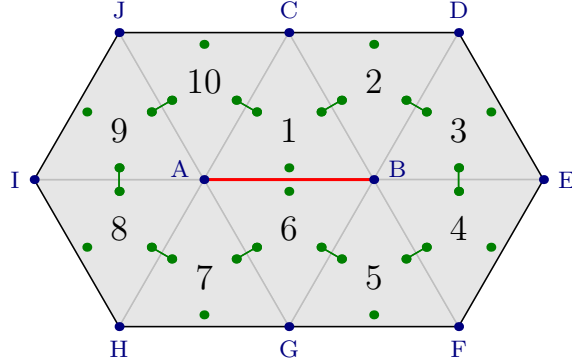


Figure 3: Graphical representation of the generalized mesh \mathcal{M}_1^* of Example 1. The adjacency graph $\mathcal{G}_{\mathcal{M}_1^*}$ is shown in green. The dot in the element i and near the edge E is associated to the split facet $(E, i) \in \mathbb{F}(\mathcal{M}_1^*)$. Even though the elements 1 and 6 have the edge AB (highlighted in red) in common, they are not adjacent.

There are $3 \times 10 = 30$ split facets (green dots in Figure 3), the first few are given by

$$\mathbb{F}(\mathcal{M}_1^*) = \{(AB, 1), (BC, 1), (AC, 1), (BC, 2), (CD, 2), (BD, 2), \dots\}.$$

The adjacency graph (represented in green in Figure 3) can be summarized by

$$1 \xleftrightarrow{BC} 2 \xleftrightarrow{BD} 3 \xleftrightarrow{BE} 4 \xleftrightarrow{BF} 5 \xleftrightarrow{BG} 6 \xleftrightarrow{AG} 7 \xleftrightarrow{AH} 8 \xleftrightarrow{AI} 9 \xleftrightarrow{AH} 10 \xleftrightarrow{AC} 1.$$

The elements 1 and 6 are not adjacent, although the triangles $\mathcal{K}(1)$ and $\mathcal{K}(6)$ share the edge AB. This creates the “fracture”, highlighted in red.

Example 2 (Two-sided segment). One can consider the generalized edge mesh \mathcal{M}_2^* (see Figure 4) with

$$\mathcal{V} = \{A, B\}, \quad \mathbf{K} = \{1, 2\}$$

with the realization $\mathcal{K}(1) = \mathcal{K}(2) = AB$. In this example, there are 4 split facets:

$$\mathbb{F}(\mathcal{M}_2^*) = \{(A, 1), (B, 1), (A, 2), (B, 2)\}$$

and the adjacency graph (represented in green in Figure 4) is given by $1 \xleftrightarrow{A} 2 \xleftrightarrow{B} 1$.

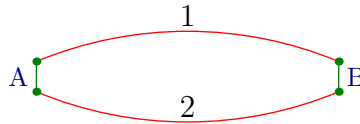


Figure 4: Graphical representation of the generalized mesh \mathcal{M}_2^* of Example 2, where the two red curves, supposed to be two instances of the segment AB, should be on top of each other. They have been torn apart to visualize the adjacency graph, represented in green.

The two elements of \mathcal{M}_2^* can be thought of as the upper and lower sides of the segment AB. They are adjacent through both of their vertices. We shall see in that this generalized mesh is one of the components of the boundary of the generalized mesh \mathcal{M}_1^* from the previous example.

2.3 Data structures

We represent generalized meshes in Matlab using the following data structure:

```

classdef GeneralizedMesh

    properties
        vtx;           % List of vertices of size Nvtx
        elt;           % Nelt x (n+1) array with entries in {1,...,Nvtx}
        nei_elt;      % Nelt x (n+1) array with entries in {0,...,Nelt}
        nei_fct;      % Nelt x (n+1) array with entries in {0,...,n+1}
    end

```

The attribute `elt` is used as in the `msh` class, except this time, the rows of `elt` are not necessarily mutually distinct. An instance of `GeneralizedMesh` represents a generalized mesh with elements $\{1, \dots, N_{elt}\}$. The i -th line of `elt` encodes the simplex attached to the element i . The adjacency graph is encoded by the attributes `nei_elt`, `nei_fct` with the following conventions:

$$\begin{aligned}
 i \xleftrightarrow{F} j &\iff \begin{cases} (\text{nei_elt}[i, \alpha], \text{nei_fct}[i, \alpha]) = (j, \beta), \\ F_\alpha(i) = F_\beta(j) = F, \end{cases} \\
 i \xleftrightarrow{F} \perp &\iff \begin{cases} (\text{nei_elt}[i, \alpha], \text{nei_fct}[i, \alpha]) = (0, 0), \\ F_\alpha(i) = F. \end{cases} \\
 &\text{for all } i, j \in \{1, \dots, N_{elt}\}.
 \end{aligned}$$

Here, for $\alpha \in \{1, \dots, n+1\}$, $F_\alpha(i)$ denotes the facet of the simplex attached to the element i , obtained by removing the vertex in position α in the i -th line of `elt`.

The d -subsimpllices of a generalized mesh \mathcal{M}^* are computed by removing duplicate entries in the list of all subsimpllices of all elements. This is done by first sorting the list of subsimpllices lexicographically (according to the vertex indices), and then removing duplicates in a second, linear pass. Hence, the number of operations required is proportional to $N_1 \log N_1$, where

$$N_1 := \binom{n}{d} \text{Card}(\mathbf{K}_{\mathcal{M}^*}) . \tag{16}$$

One of the class constructors for `GeneralizedMesh` is an implementation of Definition 4. Called on a non-branching mesh \mathcal{M} , it outputs a generalized mesh \mathcal{M}^* representing \mathcal{M} . This involves the computation of the adjacency graph of \mathcal{M} , which requires a number of operations proportional to $\text{Card}(\mathcal{M})$, the proportionality constant depending polynomially on n .

For more details, the reader is invited to consult our Matlab implementation included as supplementary material.

2.4 Generalized subfacets

The generalized d -subfacets defined in this section play an important role in the remainder of this work.

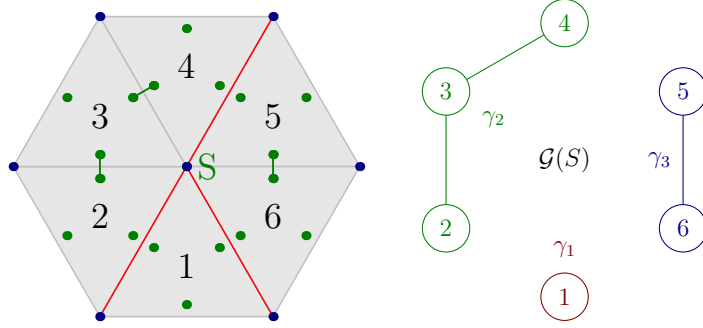


Figure 5: Possible configuration of the generalized star of a vertex S , with the same conventions as in Figure 3 (left), and corresponding graph $\mathcal{G}(S)$ (right). In this example, there are three generalized vertices attached to S : $(S, \{1\})$, $(S, \{2, 3, 4\})$ and $(S, \{5, 6\})$.

Given $S \in \sigma(\mathcal{M}^*)$, the *generalized star* of S is defined by

$$\text{st}(S, \mathcal{M}^*) := \{\mathbf{k} \in \mathcal{M}^* \mid S \in \sigma(\mathbf{k})\}. \quad (17)$$

Let $\mathcal{G}(S)$ be the graph between the elements of $\text{st}(S, \mathcal{M}^*)$, with an edge between \mathbf{k} and \mathbf{k}' if $\mathbf{k} \xleftrightarrow{S} \mathbf{k}'$ (see Figure 5). The connected components of $\mathcal{G}(S)$ define a partition $\gamma_1, \dots, \gamma_Q$ of $\text{st}(S, \mathcal{M}^*)$, and we write $\mathcal{C}(S) := \{\gamma_1, \dots, \gamma_Q\}$.

Definition 6 (Generalized subfacets). For $0 \leq d \leq n$, a *generalized d -subfacet* is a d -simplex $S \in \sigma_d(\mathcal{M}^*)$ labeled by a component $\gamma \in \mathcal{C}(S)$. The set of generalized d -subfacets, denoted by $\mathbf{S}_d(\mathcal{M}^*)$, is thus

$$\mathbf{S}_d(\mathcal{M}^*) := \{\mathbf{s} = (S, \gamma) \mid S \in \sigma_d(\mathcal{M}^*), \gamma \in \mathcal{C}(S)\}. \quad (18)$$

We say that a generalized d -subfacet $\mathbf{s} = (S, \gamma)$ is *attached to* the subsimplex S , and we extend the meaning of the realization \mathcal{K} so that $\mathcal{K}(\mathbf{s}) := S$. Also, let us write

$$\sigma_d(\mathbf{s}) := \sigma_d(S), \quad \text{st}(\mathbf{s}, \mathcal{M}^*) := \gamma.$$

A generalized d -subfacet is called a *generalized vertex* and a *generalized facet* for $d = 0$ and $d = n - 1$, respectively. We again adopt a special notation for the set of generalized facets:

$$\mathbf{F}(\mathcal{M}^*) := \mathbf{S}_{n-1}(\mathcal{M}^*). \quad (19)$$

For an n -dimensional gen-mesh \mathcal{M}^* , when $K \in \sigma_n(\mathcal{M}^*)$, the graph $\mathcal{G}(K)$ has no edges. Indeed, the elements in $\text{st}(K, \mathcal{M}^*)$ can only be adjacent through simplices of dimension $d \leq n - 1$, hence, not through K . Therefore,

$$\mathbf{S}_n(\mathcal{M}^*) \simeq \sigma_n(\mathcal{M}^*) = \mathbf{K}_{\mathcal{M}^*},$$

and we identify elements with generalized n -subfacets. When \mathcal{M}^* represents a regular mesh, then $\mathbf{S}_d(\mathcal{M}^*) \simeq \sigma_d(\mathcal{M}^*)$ for all $0 \leq d \leq n$ because of Lemma 3.

One can compute all the generalized d -subfacets of \mathcal{M}^* in a number of operations proportional

to $N_1 \log N_1 + N_2 N_3$ where

$$N_2 = \text{Card}(\sigma_d(\mathcal{M}^*)), \quad N_3 = \max_{S \in \sigma_d(\mathcal{M}^*)} \text{Card}(\text{st}(S, \mathcal{M}^*)),$$

and where N_1 is defined in Eq. (16). This is achieved by a standard graph exploration, summarized in Algorithms 1 and 2.

Algorithm 1 GeneralizedSubfacets(\mathcal{M}^*, d)

INPUTS: Generalized mesh \mathcal{M}^* , subfacet dimension d .

RETURNS: The set of generalized d -subfacets of \mathcal{M}^* , $\mathbf{S}_d(\mathcal{M}^*)$.

```

 $\mathcal{S}_d \leftarrow \{\}$  % Initialization
FOR  $S \in \sigma_d(\mathcal{M}^*)$  % Loop over the  $d$ -simplices of  $\mathcal{M}^*$ 
   $l \leftarrow \text{st}(S, \mathcal{M}^*)$ ; % Generalized star of  $S$ 
  WHILE ( $l \neq \{\}$ )
    Choose  $\mathbf{k} \in l$ ; % Pick element of the star of  $S$  not already visited
     $\gamma \leftarrow \{\}$ ;
     $(\gamma, l) \leftarrow \text{AUX}(\mathcal{M}^*, S, \gamma, l, \mathbf{k})$ ; % Visit component of  $\mathbf{k}$  and store it in  $\gamma$ .
     $\mathbf{s} \leftarrow (S, \gamma)$ ; % Create the corresponding new generalized facet
     $\mathcal{S}_d \leftarrow \mathcal{S}_d \cup \{\mathbf{s}\}$ ; % Append it to the list  $\mathcal{S}_d$ 
  END WHILE
RETURN  $\mathcal{S}_d$ 

```

Algorithm 2 AUX($\mathcal{M}^*, S, \gamma, l, \mathbf{k}$)

INPUTS: A generalized mesh \mathcal{M}^* , a simplex $S \in \sigma(\mathcal{M}^*)$, two disjoint subsets γ and l of $\text{st}(S, \mathcal{M}^*)$, an element $\mathbf{k} \in l$.

RETURNS The set γ augmented with all elements in the same component as \mathbf{k} in $\mathcal{G}(S)$, and the set l from which those elements have been removed.

```

 $\gamma \leftarrow \gamma \cup \{\mathbf{k}\}$ ; % Append element  $\mathbf{k}$  to  $\gamma$ 
 $l \leftarrow l \setminus \{\mathbf{k}\}$ ; % Remove element  $\mathbf{k}$  from  $l$ 
FOR  $F \in \mathcal{F}(\mathbf{k})$  such that  $S \in \sigma(F)$  % Loop over the facets of  $\mathbf{k}$  incident to  $S$ 
   $\mathbf{k}' \leftarrow \mathcal{N}(\mathbf{k}, F)$  % Neighbor of  $\mathbf{k}$  through  $F$ 
  IF  $\mathbf{k}' \in l$ 
     $(\gamma, l) \leftarrow \text{AUX}(\mathcal{M}^*, S, \gamma, l, \mathbf{k}')$ ; % Recursively visit neighbors of  $\mathbf{k}'$  through  $S$ 
  END IF
END FOR
RETURN  $(\gamma, l)$ 

```

Definition 7 (Incidence and adjacency of generalized subfacets). Given $\mathbf{s}, \mathbf{s}' \in \mathbf{S}_{d'}(\mathcal{M}^*)$, with $0 \leq d < d' \leq n$, we write $\mathbf{s} \subset \mathbf{s}'$ if

$$\mathcal{K}(\mathbf{s}) \subset \mathcal{K}(\mathbf{s}') \text{ and } \text{st}(\mathbf{s}, \mathcal{M}^*) \supset \text{st}(\mathbf{s}', \mathcal{M}^*),$$

in which case we say that \mathbf{s} is contained in \mathbf{s}' . When $|d - d'| = 1$, we say that \mathbf{s} and \mathbf{s}' are incident. Two generalized d -subfacets are adjacent if they are incident to a common generalized $(d - 1)$ -subfacet.

For $d = n$, this new notion of adjacency is consistent with the previous one:

Lemma 4. *Two elements $\mathbf{k}, \mathbf{k}' \in \mathbf{K}_{\mathcal{M}^*}$ are adjacent in the sense of Definition 1 if and only if they are adjacent in the sense of Definition 7.*

Proof. If $\mathbf{k} \xleftrightarrow{F} \mathbf{k}'$, then there is a genfacet $\mathbf{f} \in \mathbf{F}(\mathcal{M}^*)$, with $\{\mathbf{k}, \mathbf{k}'\} \subset \text{st}(\mathbf{f}, \mathcal{M}^*)$. But this implies that \mathbf{k} and \mathbf{k}' are both incident to \mathbf{f} .

Conversely, if \mathbf{k} and \mathbf{k}' are both incident to a facet \mathbf{f} attached to a simplex F , then $\{\mathbf{k}, \mathbf{k}'\} \subset \text{st}(\mathbf{f}, \mathcal{M}^*)$, so by definition of $\mathcal{G}(F)$, $\mathbf{k} \xleftrightarrow{F} \mathbf{k}'$. \square

Lemma 5. *Let \mathbf{k} and \mathbf{k}' be elements of a generalized mesh, and let $\mathbf{V}(\mathbf{k})$ and $\mathbf{V}(\mathbf{k}')$ be the set of generalized vertices contained in \mathbf{k} and \mathbf{k}' , respectively. If $\mathbf{k} \xleftrightarrow{F} \mathbf{k}'$, then*

$$\forall V \in \sigma_0(F), \exists \mathbf{v} \in \mathbf{V}(\mathbf{k}) \cap \mathbf{V}(\mathbf{k}') : \mathcal{K}(\mathbf{v}) = V.$$

In words, for each vertex V of F , there is a generalized vertex \mathbf{v} attached to V , and contained both in \mathbf{k} and in \mathbf{k}' . As a consequence, two adjacent elements share at least n distinct generalized vertices.

Proof. Write $F = \{V_1, V_2, \dots, V_n\}$. For each $k \in \{1, \dots, n\}$, since $V_k \in \sigma(F)$ one has

$$\mathbf{k} \xleftrightarrow{V_k} \mathbf{k}'.$$

Hence, there is a component $\gamma_k \in \mathcal{C}(V_k)$ containing both \mathbf{k} and \mathbf{k}' . Set $\mathbf{v}_k := (V_k, \gamma_k) \in \mathbf{S}_0(\mathcal{M}^*)$. Then, the generalized vertices $\mathbf{v}_1, \dots, \mathbf{v}_n$ all belong to both \mathbf{k} and \mathbf{k}' . \square

Example 3 (Domain with a crack). We consider again the generalized mesh \mathcal{M}_1^* introduced in Example 1, see Figure 3. The generalized vertices are

$$\begin{aligned} \mathbf{a} &= (A, \{6, 7, 8, 9, 10, 1\}), \quad \mathbf{b} = (B, \{1, 2, 3, 4, 5, 6\}), \\ \mathbf{c} &= (C, \{1, 2, 10\}), \quad \mathbf{d} = (D, \{2, 3\}), \quad \mathbf{e} = (E, \{3, 4\}), \quad \mathbf{f} = (F, \{4, 5\}), \\ \mathbf{g} &= (G, \{5, 6, 7\}), \quad \mathbf{h} = (H, \{7, 8\}), \quad \mathbf{i} = (I, \{8, 9\}), \quad \mathbf{j} = (J, \{9, 10\}). \end{aligned}$$

In this case, $\text{Card}(\sigma_0(\mathcal{M}_1^*)) = \text{Card}(\mathbf{S}_0(\mathcal{M}_1^*))$. However, we have

$$\text{Card}(\mathbf{S}_1(\mathcal{M}_1^*)) = \text{Card}(\sigma_1(\mathcal{M}_1^*)) + 1,$$

as there are two generalized edges attached to the segment AB, namely

$$\mathbf{e}_1 := (AB, \{1\}), \quad \mathbf{e}_2 := (AB, \{6\}).$$

They can be interpreted as the top and bottom sides, respectively, of the segment AB.

Remark 1. *In the previous example, we see that the elements 1 and 6 share the two generalized vertices \mathbf{a} and \mathbf{b} , but they are not adjacent. This shows that the converse of the last statement in Lemma 5 above, is false.*

Example 4. We consider the generalized mesh \mathcal{M}_3^* represented in Figure 6 below. It represents a rectangular domain Ω containing a fracture Γ (red edges in the figure). The main merit of this example is to show an instance of a generalized mesh with “split nodes”, as there are 4 generalized vertices attached to the vertex O :

$$\mathbf{o}_1 = (O, \{11, 12\}), \quad \mathbf{o}_2 = (O, \{14\}), \quad \mathbf{o}_3 = (O, \{19\}), \quad \text{and} \quad \mathbf{o}_4 = (O, \{21, 22\}).$$

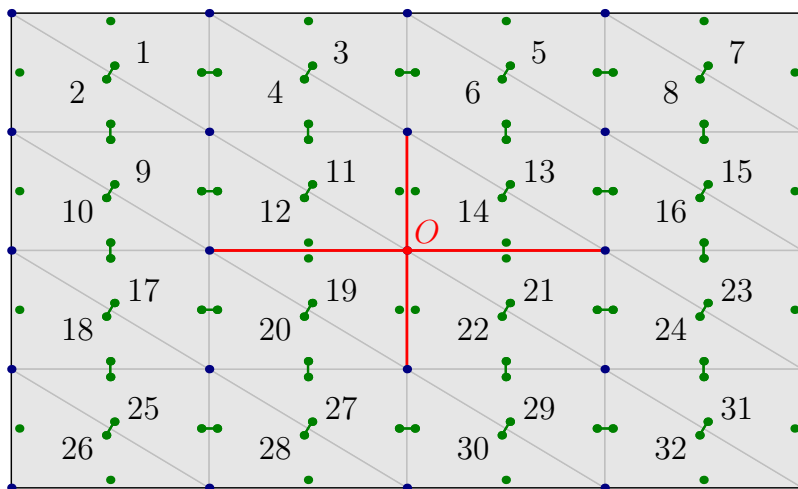


Figure 6: A generalized mesh representing a domain with a cross-shaped fracture, with the same conventions as in Figure 3.

3 Boundary of a generalized mesh

In this section, we define the boundary $\partial^* \mathcal{M}^*$ of a generalized mesh \mathcal{M}^* , in a way that generalizes the boundary of regular meshes.

Recall the definition of the set of split facets $\mathbb{F}(\mathcal{M}^*)$ from Eq. (12) and the neighbor function \mathcal{N} from Eq. (14). In what follows, $\mathbf{F}_b(\mathcal{M}^*)$ denotes the set of *boundary split facets* of \mathcal{M}^* , defined by

$$\mathbf{F}_b(\mathcal{M}^*) := \{(F, \mathbf{k}) \in \mathbb{F}(\mathcal{M}^*) \mid \mathcal{N}(\mathbf{k}, F) = \perp\}, \quad (20)$$

that is, the set of nodes of degree 0 in the adjacency graph $\mathcal{G}_{\mathcal{M}^*}$.

The set $\mathbf{F}_b(\mathcal{M}^*)$ will be the set of elements of $\partial^* \mathcal{M}^*$. Our main task is now to define a suitable adjacency graph $\mathcal{G}_{\partial^* \mathcal{M}^*}$, which amounts to specifying the adjacency relations among elements of $\mathbf{F}_b(\mathcal{M}^*)$. The key idea is illustrated in Figure 7. Given two split facets

$$\mathbf{f} = (F, \mathbf{k}), \quad \mathbf{f}' = (F', \mathbf{k}')$$

such that F and F' share a common facet S , we will declare that \mathbf{f} and \mathbf{f}' are adjacent through S if they can be linked by a chain of adjacent elements through S .

We now describe this idea more precisely.

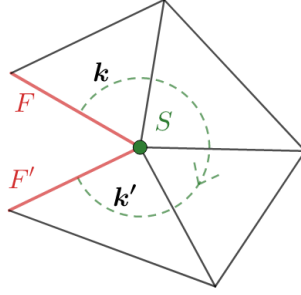


Figure 7: Sketch of the idea for the definition of the adjacency relation in the generalized boundary.

Lemma 6. *Let \mathcal{M}^* be an n -dimensional generalized mesh, $n \geq 2$, and let $(F, \mathbf{k}) \in \mathbf{F}_b(\mathcal{M}^*)$. For each $S \in \mathcal{F}(F)$, there exists a unique sequence $\{\mathbf{k}_q\}_{1 \leq q \leq Q} \subset \mathbf{K}_{\mathcal{M}^*}$ of distinct elements, and a unique sequence $\{F_q\}_{0 \leq q \leq Q} \subset \mathcal{F}(\mathcal{M}^*)$ of distinct facets, all containing S , such that $\mathbf{k} = \mathbf{k}_1$, $F = F_0$, and*

$$\perp \xleftrightarrow{F_0} \mathbf{k}_1 \xleftrightarrow{F_1} \mathbf{k}_2 \xleftrightarrow{F_2} \dots \xleftrightarrow{F_{Q-2}} \mathbf{k}_{Q-1} \xleftrightarrow{F_{Q-1}} \mathbf{k}_Q \xleftrightarrow{F_Q} \perp .$$

Proof. Let $\mathbf{k}_1 := \mathbf{k}$, $F_0 := F$, and let F_1 be the unique facet of \mathbf{k} , distinct from F , containing S . If $\mathcal{N}(\mathbf{k}, F_1) = \perp$, then

$$\perp \xleftrightarrow{F_0} \mathbf{k}_1 \xleftrightarrow{F_1} \perp ,$$

and there is nothing left to prove.

Otherwise, let $\mathbf{k}_2 := \mathcal{N}(\mathbf{k}_1, F_1)$, and let the construction be continued recursively in the following way: \mathbf{k}_i and F_{i-1} being defined, let F_i be the facet of \mathbf{k}_i , distinct from F_{i-1} , and containing S . If

$$\mathcal{N}(\mathbf{k}_i, F_i) = \perp ,$$

then stop with $Q = i$. Otherwise, let

$$\mathbf{k}_{i+1} = \mathcal{N}(\mathbf{k}_i, F_i) .$$

Let us show by induction that for each j such that \mathbf{k}_j is defined, the elements $\mathbf{k}_1, \dots, \mathbf{k}_j$ are all distinct. For $j = 2$, this follows from the requirement (ii) of Definition 1, i.e. that

$$\mathbf{k} \xleftrightarrow{F} \mathbf{k}' \implies \mathbf{k} \neq \mathbf{k}' . \quad (21)$$

Next, assuming that it is true for some $j \geq 2$, and if \mathbf{k}_{j+1} is defined, let us show by contradiction that $\mathbf{k}_{j+1} \notin \{\mathbf{k}_i\}_{1 \leq i \leq j}$. To this end, we assume that there exists $a < j + 1$ such that $\mathbf{k}_a = \mathbf{k}_{j+1}$. The situation is then summarized by the diagram below.

$$\begin{array}{ccc} & \mathbf{k}_a & \xleftrightarrow{F_a} & \mathbf{k}_{a+1} \\ & & \parallel & \\ \mathbf{k}_j & \xleftrightarrow{F_j} & & \mathbf{k}_{j+1} \end{array}$$

Note that $\mathbf{k}_{a+1} \neq \mathbf{k}_{j+1}$, again by the property (21) above. Consequently, $a \neq j$, so either $a < j - 1$ or $a = j - 1$.

On the one hand, if we assume that $a < j - 1$, then \mathbf{k}_{a+1} and \mathbf{k}_j are two distinct neighbors of \mathbf{k}_a through F_a and F_j , respectively. Hence, $F_j \neq F_a$ so that $F_{a-1} = F_j$ and therefore

$$\mathcal{N}(\mathbf{k}_a, F_{a-1}) = \mathbf{k}_j \neq \perp .$$

This implies that $a \geq 2$, and $\mathbf{k}_j = \mathbf{k}_{a-1}$, which is in contradiction with the induction hypothesis.

On the other hand, assume that $a = j - 1$. We now face the situation represented in the diagram below.

$$\mathbf{k}_{j-1} \xleftrightarrow{F_{j-1}} \mathbf{k}_j \xleftrightarrow{F_j} \mathbf{k}_{j+1} = \mathbf{k}_{j-1}$$

By definition of F_j , we have $F_j \neq F_{j-1}$, and because of the situation above, both are faces of the simplex attached to \mathbf{k}_{j-1} . Hence, we must have $F_{j-2} = F_j$, and therefore

$$\mathcal{N}(\mathbf{k}_{j-1}, F_{j-2}) = \mathbf{k}_j \neq \perp .$$

This means that \mathbf{k}_{j-2} is defined and equal to \mathbf{k}_j , leading to a contradiction also in this case. The existence of a is therefore contradictory, concluding the induction.

Having established that the sequence of elements generated by this process has no repetition, we conclude that it must be finite, since \mathcal{M}^* only has a finite number of elements. With this, the existence of the chain is proved. The fact that the chain is unique follows immediately from the axiom (i) of the adjacency graph in Definition 1. \square

Hence for each boundary split facet $\mathbf{f} := (F, \mathbf{k}) \in \mathbf{F}_b(\mathcal{M}^*)$, and for each facet S of F , there is a finite and unique ‘‘chain of elements’’ starting from this boundary split facet and circling around S . The opposite end of this chain, $\mathbf{f}' := (F_Q, \mathbf{k}_Q)$ is again a boundary split facet, and we deem it the neighbor of \mathbf{f} through S . We write

$$\mathcal{N}_b(\mathbf{f}, S) := \mathbf{f}' .$$

Corollary 1. *The function \mathcal{N}_b satisfies*

$$\forall \mathbf{f} \in \mathbf{F}_b(\mathcal{M}^*), \forall S \in \mathcal{F}(F), \quad \mathcal{N}_b(\mathbf{f}, S) \neq \mathbf{f} \quad \text{and}$$

$$\mathcal{N}_b(\mathbf{f}, S) = \mathbf{f}' \iff \mathcal{N}_b(\mathbf{f}', S) = \mathbf{f} .$$

Definition 8 (Generalized boundary). Given an n -dimensional generalized mesh \mathcal{M}^* , with $n \geq 1$, the *generalized boundary* (or simply boundary) of \mathcal{M}^* is the $(n - 1)$ -dimensional generalized mesh $\partial^* \mathcal{M}^*$ with

- the vertex set $\mathcal{V}_{\partial^* \mathcal{M}^*} := \mathcal{V}_{\mathcal{M}^*}$,
- the elements $\mathbf{K}_{\partial^* \mathcal{M}^*} := \mathbf{F}_b(\mathcal{M}^*)$,
- the realization $\mathcal{K}_{\partial^* \mathcal{M}^*}$, defined by $\mathcal{K}_{\partial^* \mathcal{M}^*}(\mathbf{f}) := F$ when $\mathbf{f} = (F, \mathbf{k})$.
- If $n \geq 2$, the adjacency graph $\mathcal{G}_{\partial^* \mathcal{M}^*}$ defined by

$$\mathbf{f} \xleftrightarrow[\partial^* \mathcal{M}^*]{S} \mathbf{f}' \iff \mathcal{N}_b(\mathbf{f}, S) = \mathbf{f}' .$$

If \mathcal{M}^* is a 0-dimensional generalized mesh, we set $\partial^* \mathcal{M}^* := \emptyset$.

This definition respects the axioms of generalized meshes by Corollary 1.

Example 5. Consider again the generalized mesh \mathcal{M}_3^* represented in Figure 6. Its generalized boundary is represented in Figure 8 below, where the inner component of the boundary (in red) has been “inflated” to help visualizing the adjacency structure.

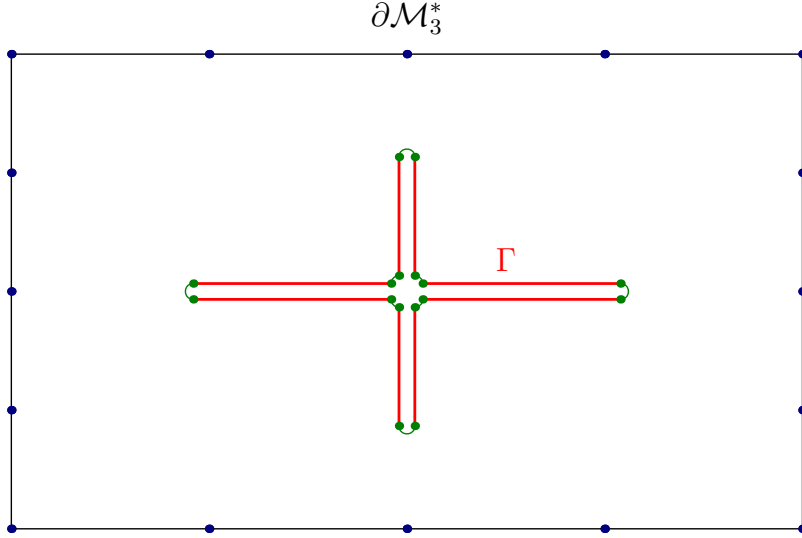


Figure 8: Sketch of the generalized boundary of \mathcal{M}_3^* , as shown in Figure 6.

Now, we prove that the previous definition suitably generalizes the notion of boundary for regular meshes.³ For the terminology used in the next lemma, recall Definitions 3 and 4:

Lemma 7. *Let \mathcal{M} be a regular mesh, and let \mathcal{M}^* (resp. $(\partial\mathcal{M})^*$) be the generalized mesh representing \mathcal{M} (resp. $\partial\mathcal{M}$). Then, the meshes $\partial^* \mathcal{M}^*$ and $(\partial\mathcal{M})^*$ are equal, up to a relabeling.*

Proof. Given $F \in \partial\mathcal{M}$, there exists a unique element $K \in \mathcal{M}$ incident to F , and it satisfies

$$K \xleftrightarrow[\mathcal{M}]{F} \perp .$$

Hence, $(F, K) \in \mathbf{F}_b(\mathcal{M}^*)$, and we write $(F, K) =: \varphi(F)$. Since $\mathbf{K}_{(\partial\mathcal{M})^*} = \partial\mathcal{M}$ and $\mathbf{K}_{\partial^* \mathcal{M}^*} = \mathbf{F}_b(\mathcal{M}^*)$, this gives a bijection

$$\varphi : \mathbf{K}_{(\partial\mathcal{M})^*} \rightarrow \mathbf{K}_{\partial^* \mathcal{M}^*} .$$

Obviously, there holds $\mathcal{K}_{(\partial\mathcal{M})^*} = \mathcal{K}_{\partial^* \mathcal{M}^*} \circ \varphi$. Moreover, given $F, F' \in \mathbf{K}_{(\partial\mathcal{M})^*}$, assume that

$$F \xleftrightarrow[(\partial\mathcal{M})^*]{S} F' .$$

³We cannot formulate Lemma 7 in general for non-branching triangulations, since they can have branching boundaries – for which there is no corresponding generalized mesh, see the remark below Definition 4.

Let K and K' be such that $\varphi(F) = (F, K)$ and $\varphi(F') = (F', K')$. Both K and K' are in the star of S . Therefore, by Lemma 3, there exists K_1, \dots, K_Q in the star of S , with $K_1 = K$, $K_Q = K'$, such that

$$K_1 \xleftarrow[\mathcal{M}]{F_1} K_2 \xleftarrow[\mathcal{M}]{F_2} K_3 \xleftarrow[\mathcal{M}]{F_3} \dots \xleftarrow[\mathcal{M}]{F_{Q-2}} K_{Q-1} \xleftarrow[\mathcal{M}]{F_{Q-1}} K_Q,$$

with $F_i := K_i \cap K_{i+1}$, $1 \leq i \leq Q-1$. Furthermore, we have

$$\perp \xleftarrow[\mathcal{M}]{F} K, \quad K' \xleftarrow[\mathcal{M}]{F'} \perp.$$

By definition of \mathcal{M}^* , it follows that

$$\perp \xleftarrow[\mathcal{M}^*]{F} K \xleftarrow[\mathcal{M}^*]{F_1} K_2 \xleftarrow[\mathcal{M}^*]{F_3} \dots \xleftarrow[\mathcal{M}^*]{F_{Q-2}} K_{Q-1} \xleftarrow[\mathcal{M}^*]{F_{Q-1}} K' \xleftarrow[\mathcal{M}^*]{F'} \perp,$$

that is to say

$$(F', K') = \mathcal{N}_b((F, K), S).$$

We have thus shown

$$F \xleftarrow[\partial\mathcal{M}^*]{S} F' \implies \varphi(F) \xleftarrow[\partial^*\mathcal{M}^*]{S} \varphi(F').$$

The reverse implication is immediate. Hence $\partial^*\mathcal{M}^*$ is a relabeling of $(\partial\mathcal{M})^*$. \square

From now on, we drop the star from ∂^* . The following result is a direct consequence of the definition:

Lemma 8. *Given a generalized mesh \mathcal{M}^* , the generalized mesh $\partial\mathcal{M}^*$ is empty.*

Definition 9 (Induced orientation on the boundary of a generalized mesh). Let \mathcal{M}^* be an n -dimensional generalized mesh, with $n \geq 1$, equipped with some (possibly non-compatible) orientation. We define an orientation of $\partial\mathcal{M}^*$ as follows: for each element $\mathbf{f} = (F, \mathbf{k}) \in \mathbf{F}_b(\mathcal{M}^*)$ of \mathcal{M}^* , we choose

$$[\mathbf{f}]_{\partial\mathcal{M}^*} := [F]_{[K]}$$

where K is the simplex attached to \mathbf{k} , $[K] = [\mathbf{k}]_{\mathcal{M}^*}$ is fixed by the orientation of \mathcal{M}^* , and $[F]_{[K]}$ is defined by Eq. (2). This orientation of $\partial\mathcal{M}^*$ is called the orientation *induced by \mathcal{M}^** .

The next result shows that the boundary of an orientable generalized mesh is orientable.

Lemma 9. *If the orientation of \mathcal{M}^* is compatible, then the induced orientation of $\partial\mathcal{M}^*$ is compatible.*

Proof. Let \mathcal{M}^* be a generalized mesh equipped with a compatible orientation. Consider two elements $\mathbf{f} = (F, \mathbf{k})$ and $\mathbf{f}' = (F', \mathbf{k}')$ such that

$$\mathbf{f} \xleftarrow[\partial\mathcal{M}^*]{S} \mathbf{f}'.$$

We may introduce the chain

$$\perp \xleftarrow[\mathcal{M}^*]{F_0} \mathbf{k}_1 \xleftarrow[\mathcal{M}^*]{F_1} \mathbf{k}_2 \xleftarrow[\mathcal{M}^*]{F_2} \dots \xleftarrow[\mathcal{M}^*]{F_{Q-2}} \mathbf{k}_{q-1} \xleftarrow[\mathcal{M}^*]{F_{Q-1}} \mathbf{k}_Q \xleftarrow[\mathcal{M}^*]{F_Q} \perp, \quad (22)$$

where $F_0 = F$, $\mathbf{k}_1 = \mathbf{k}$, $F_Q = F'$ and $\mathbf{k}_Q = \mathbf{k}'$. We define

$$\begin{aligned} [F_q]_{\text{left}} &:= \text{orientation of } F_q \text{ induced by } [\mathbf{k}_q]_{\mathcal{M}^*} & q \in \{1, \dots, Q\}, \\ [F_q]_{\text{right}} &:= \text{orientation of } F_q \text{ induced by } [\mathbf{k}_{q+1}]_{\mathcal{M}^*} & q \in \{0, \dots, Q-1\}. \end{aligned}$$

On the one hand, by Lemma 1, it holds that

$$\forall q \in \{1, \dots, Q\}, \quad [F_{q-1}]_{\text{right}} \text{ and } [F_q]_{\text{left}} \text{ induce opposite orientations on } S,$$

On the other hand, by the property that $[\mathbf{k}_q]_{\mathcal{M}^*}$ and $[\mathbf{k}_{q+1}]_{\mathcal{M}^*}$ are consistently oriented (since the orientation of \mathcal{M}^* is compatible), it holds that

$$\forall q \in \{1, \dots, Q-1\}, \quad [F_q]_{\text{right}} = -[F_q]_{\text{left}},$$

Consequently, $[F_q]_{\text{left}}$ and $[F_q]_{\text{right}}$ also induce opposite orientations on S .

It results from those two facts that $[F_0]_{\text{right}}$ and $[F_Q]_{\text{left}}$ induce opposite orientations on S , so they are consistently oriented. The conclusion of the lemma follows once we notice that $[F_0]_{\text{left}}$ and $[F_Q]_{\text{left}}$ are nothing else than the orientations of F and F' fixed by the orientation induced by \mathcal{M}^* on $\partial\mathcal{M}^*$ according to Definition 9. \square

4 Fractured meshes and virtual inflation

In this section, we focus on one particular kind of generalized mesh: those obtained, starting from a regular mesh \mathcal{M}_Ω , by dropping the adjacency between selected pairs of neighbor simplices, see below for a more precise definition. The set of facets shared by those selected pairs, \mathcal{M}_Γ , is called the fracture. Particular examples of such meshes have already been encountered in Example 1 and Example 4.

We are interested in the generalized boundaries of those ‘‘fractured meshes’’. The main goal of this section is to provide an algorithm that reconstructs the generalized boundary efficiently from the fracture mesh \mathcal{M}_Γ alone, i.e. without relying on the external regular mesh \mathcal{M}_Ω .

4.1 Fractured meshes

Consider a regular mesh \mathcal{M}_Ω of dimension $n \geq 2$ and let $\Omega := |\mathcal{M}|$. Let $\mathcal{M}_\Gamma \subset \mathcal{F}(\mathcal{M}_\Omega)$ be a (not necessarily regular) simplicial mesh of dimension $n-1$, called the fracture, and let $\Gamma := |\mathcal{M}_\Gamma|$. For example, if $n = 3$, \mathcal{M}_Γ may be the mesh represented in Figure 1.

Definition 10 (Fractured mesh). Given \mathcal{M}_Ω and \mathcal{M}_Γ fulfilling the conditions above, the *fractured mesh* $\mathcal{M}_{\Omega \setminus \Gamma}^*$ is the generalized mesh with

- the vertex set $\mathcal{V}_{\mathcal{M}_{\Omega \setminus \Gamma}^*} := \sigma_0(\mathcal{M}_\Omega)$,
- the elements $\mathbf{K}_{\mathcal{M}_{\Omega \setminus \Gamma}^*} := \mathcal{M}_\Omega$,
- the identity realization $\mathcal{K}_{\mathcal{M}_{\Omega \setminus \Gamma}^*}$ i.e. $\forall K \in \mathcal{M}_\Omega, \mathcal{K}_{\mathcal{M}_{\Omega \setminus \Gamma}^*}(K) = K$,

- the adjacency graph defined by

$$K \xleftrightarrow[\mathcal{M}_{\Omega \setminus \Gamma}^*]{F} K' \iff \left(K \xleftrightarrow[\mathcal{M}_{\Omega}]{} K' \text{ and } F = K \cap K' \notin \mathcal{M}_{\Gamma} \right).$$

In words, two elements of $\mathcal{M}_{\Omega \setminus \Gamma}^*$ are adjacent if they share a facet F which is not in the fracture.

4.2 Extrinsic virtual inflation

Given a fractured mesh $\mathcal{M}_{\Omega \setminus \Gamma}^*$, one can consider its boundary $\partial \mathcal{M}_{\Omega \setminus \Gamma}^*$ according to Definition 8. In this paragraph, we assume that $\Gamma \cap \partial \Omega = \emptyset$. Then, some components of $\partial \mathcal{M}_{\Omega \setminus \Gamma}^*$ are in $\partial \mathcal{M}_{\Omega}$, and the remaining components give a generalized mesh that we denote by $\mathcal{M}_{\Gamma}^*(\Omega)$, and call the *extrinsic inflation* of \mathcal{M}_{Γ} via \mathcal{M}_{Ω} . More precisely:

Definition 11 (Extrinsic inflation). Given an n -dimensional regular mesh \mathcal{M}_{Ω} and a mesh

$$\mathcal{M}_{\Gamma} \subset \mathcal{F}(\mathcal{M}_{\Omega}) \setminus \partial \mathcal{M}_{\Omega},$$

the *extrinsic inflation* of \mathcal{M}_{Γ} via \mathcal{M}_{Ω} is the $(n-1)$ -dimensional generalized mesh $\mathcal{M}_{\Gamma}^*(\Omega)$ with

- the vertex set $\mathcal{V}_{\mathcal{M}_{\Gamma}^*(\Omega)} := \sigma_0(\mathcal{M}_{\Gamma})$,
- the elements $\mathbf{K}_{\mathcal{M}_{\Gamma}^*(\Omega)} := \{(F, K) \in \mathcal{M}_{\Gamma} \times \mathcal{M}_{\Omega} \mid F \in \mathcal{F}(K)\}$,
- the realization $\mathcal{K}_{\mathcal{M}_{\Gamma}^*(\Omega)}$ defined by

$$\mathcal{K}_{\mathcal{M}_{\Gamma}^*(\Omega)}((F, K)) := F$$

- the adjacency graph defined by

$$\forall \mathbf{f}, \mathbf{f}' \in \mathbf{K}_{\mathcal{M}_{\Gamma}^*(\Omega)}, \quad \mathbf{f} \xleftrightarrow[\mathcal{M}_{\Gamma}^*(\Omega)]{S} \mathbf{f}' \iff \mathbf{f} \xleftrightarrow[\partial \mathcal{M}_{\Omega \setminus \Gamma}^*]{S} \mathbf{f}',$$

where $\mathcal{M}_{\Omega \setminus \Gamma}^*$ is the fractured mesh defined in Definition 10.

Observe that $\mathbf{K}_{\mathcal{M}_{\Gamma}^*(\Omega)} \subset \mathbf{K}_{\partial \mathcal{M}_{\Omega \setminus \Gamma}^*}$, so that the definition of the adjacency graph makes sense. Furthermore, note that the assumption $\Gamma \cap \partial \Omega = \emptyset$ ensures the property

$$\forall (\mathbf{f}, \mathbf{f}') \in \partial \mathcal{M}_{\Omega \setminus \Gamma}^* \times \partial \mathcal{M}_{\Omega \setminus \Gamma}^*, \quad (\mathbf{f} \in \mathcal{M}_{\Gamma}^*(\Omega) \text{ and } \mathbf{f} \xleftrightarrow[\mathcal{M}_{\Gamma}^*(\Omega)]{S} \mathbf{f}') \implies \mathbf{f}' \in \mathcal{M}_{\Gamma}^*(\Omega).$$

For example, if $\mathcal{M}_{\Omega \setminus \Gamma}^*$ is equal to the generalized mesh \mathcal{M}_1^* of Example 1, then $\mathcal{M}_{\Gamma}^*(\Omega)$ is equal to the generalized mesh \mathcal{M}_2^* of Example 2. The idea is also represented schematically in Figure 9.

This defines a simple, purely combinatorial procedure which, on the input of a possibly non-regular mesh \mathcal{M}_{Γ} and a surrounding regular mesh \mathcal{M}_{Ω} , returns a generalized mesh $\mathcal{M}_{\Gamma}^*(\Omega)$, which is roughly speaking a two sided version of \mathcal{M}_{Γ} . As a result of this procedure, most vertices of \mathcal{M}_{Γ} are duplicated into two distinct generalized vertices, one on each “side” of the surface $|\mathcal{M}_{\Gamma}|$ (except

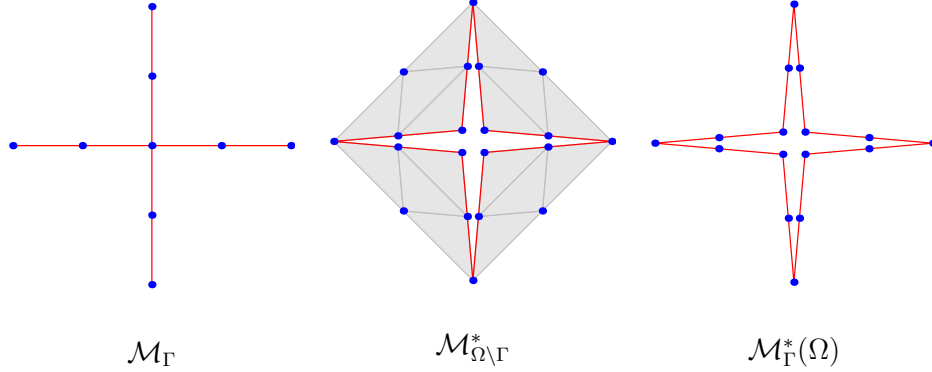


Figure 9: Schematic representation of the extrinsic inflation procedure. Starting from a possibly non-regular mesh \mathcal{M}_Γ (left panel), form the fractured mesh $\mathcal{M}_{\Omega \setminus \Gamma}^*$ using the exterior regular mesh \mathcal{M}_Ω (middle), compute its generalized boundary and return the “submesh” obtained by only keeping components corresponding to \mathcal{M}_Γ (right). The blue dots on the left (resp. right) figure represent the vertices (resp. generalized vertices) of \mathcal{M}_Γ (resp. of $\mathcal{M}_\Gamma^*(\Omega)$). As in Figure 8, a gap has been introduced in the center of the cross shape only for visualization purposes. In reality, the four central blue dots are on top of each other, and so on. On the middle figure, only a subset of the elements of \mathcal{M}_Ω is represented (gray triangles), the exterior boundary $\partial\Omega$ is not visible.

those vertices located on junction points or on the boundary, which may be multiplied into more than two copies, or not at all).

It turns out that when \mathcal{M}_Γ is an edge mesh in \mathbb{R}^2 , or a triangular mesh in \mathbb{R}^3 , $\mathcal{M}_\Gamma^*(\Omega)$ is in fact independent of \mathcal{M}_Ω up to a relabeling, and one can construct such a relabeling intrinsically, without the need for any external mesh \mathcal{M}_Ω . The construction has been sketched by two of the authors in [19, Section 4.2]. To present it more precisely, we now review some properties of oriented angles in \mathbb{R}^3 .

4.3 Oriented angles in \mathbb{R}^3

Let T_1 and T_2 be two triangles in \mathbb{R}^3 , sharing an edge. Let us denote their vertices by $\{A, B, C\}$ and $\{B, C, D\}$, respectively. We define the *geometric angle* $\Theta(T_1, T_2) \in [0, \pi)$ by

$$\cos \Theta(T_1, T_2) = \frac{\overrightarrow{OA'} \cdot \overrightarrow{OD'}}{\|\overrightarrow{OA'}\| \|\overrightarrow{OD'}\|}, \quad (23)$$

C' (resp. D') is the orthogonal projections of C (resp. D) on the plane perpendicular to \overrightarrow{BC} , through the origin O , i.e.

$$\overrightarrow{OA'} = \overrightarrow{OA} - (\overrightarrow{OA} \cdot \mathbf{u})\mathbf{u}, \quad \overrightarrow{OD'} = \overrightarrow{OD} - (\overrightarrow{OD} \cdot \mathbf{u})\mathbf{u}, \quad \mathbf{u} := \frac{\overrightarrow{BC}}{\|\overrightarrow{BC}\|}.$$

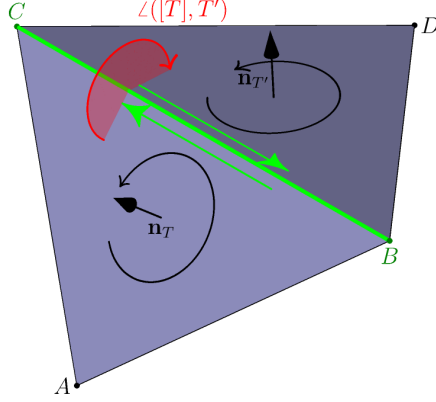


Figure 10: The triangles $[T] = [A, B, C]$ and $[T'] = [B, D, C]$ are consistently oriented. The oriented angle $\angle([T], [T'])$ is represented in red.

Given an orientation $[T_1]$ of T_1 , we define the *oriented angle* $\angle([T_1], T_2) \in (0, 2\pi]$ by

$$\angle([T_1], T_2) = \begin{cases} \Theta(T_1, T_2) & \text{if } \overrightarrow{AD} \cdot \mathbf{n}_{T_1} > 0, \\ 2\pi - \Theta(T_1, T_2) & \text{otherwise,} \end{cases} \quad (24)$$

where \mathbf{n}_{T_1} is the unit normal vector to T_1 fixed by its orientation according to Eq. (4) (see Figure 10). One has

$$\angle([T_1], T_2) = 2\pi - \angle(-[T_1], T_2). \quad (25)$$

In addition, every oriented triangle $[T]$ satisfies $\angle([T], T) = 2\pi$.

Let E_1 and E_2 be two edges in the plane sharing exactly one vertex, and let $[E_1]$ be an orientation of E_1 . Write $[E_1] = [A, B]$ and let C be the vertex of E_2 not shared by E_1 . We define $\angle([E_1], E_2)$ as the counter-clockwise measure in $(0, 2\pi)$ of the angle from \overrightarrow{AB} to \overrightarrow{AC} around A . We furthermore define $\angle([E_1], E_1) := 2\pi$. With this definition, Eq. (25) also holds for oriented angles between edges in \mathbb{R}^2 .

Lemma 10. *If $[T_1]$ and $[T_2]$ are consistently oriented triangles, then*

$$\angle([T_1], T_2) = \angle([T_2], T_1).$$

The same result holds for oriented edges.

Proof. Using the rule (25) above, we can assume without loss of generality that $T_1 = [A, B, C]$ and $T_2 = [C, B, D]$. The corresponding normal vectors are given by

$$\mathbf{n}_1 = \frac{\overrightarrow{AB} \times \overrightarrow{AC}}{\|\overrightarrow{AB} \times \overrightarrow{AC}\|}, \quad \mathbf{n}_2 = \frac{\overrightarrow{BD} \times \overrightarrow{BC}}{\|\overrightarrow{BD} \times \overrightarrow{BC}\|}.$$

By the properties of cross product, one has

$$\overrightarrow{AD} \cdot (\overrightarrow{AB} \times \overrightarrow{AC}) = \overrightarrow{DA} \cdot (\overrightarrow{BD} \times \overrightarrow{BC}).$$

We deduce that $\overrightarrow{AD} \cdot \mathbf{n}_1$ and $\overrightarrow{DA} \cdot \mathbf{n}_2$ have the same sign, and thus $\angle([T_1], T_2) = \angle([T_2], T_1)$. \square

We now state an elementary property of oriented angles in regular meshes, and an useful consequence for the next subsection.

Lemma 11. *Let $[K]$ be a naturally oriented tetrahedron in \mathbb{R}^3 , with vertices A, B, C and D . Let E be a point in \mathbb{R}^3 , and denote by T_1, T_2 and T_3 the triangles with vertices $\{A, B, C\}$, $\{B, C, D\}$ and $\{B, C, E\}$, respectively (see Figure 11). Let $[T_1]$ be the orientation of T_1 induced by $[K]$. Assume that*

$$\angle([T_1], T_3) < \angle([T_1], T_2)$$

Then T_2 intersects the interior of K , and thus

$$|T_2| \cap |K| \neq |T_2 \cap K| .$$

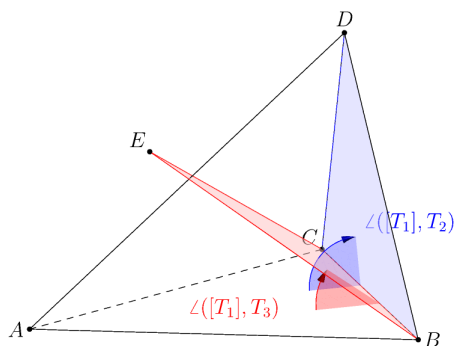


Figure 11: Configuration of Lemma 11.

Corollary 2. *Let \mathcal{M} be a regular tetrahedral mesh, let $[K]$ be a naturally oriented element of \mathcal{M} , and T_1, T_2 two of its triangular faces, sharing an edge E . Let $[T_1]$ be the orientation of T_1 induced by $[K]$. Then it holds that*

$$\forall T' \in \mathcal{F}(\mathcal{M}) \text{ s.t. } E \in \mathcal{F}(T'), \quad \angle([T_1], T') \leq \angle([T_1], T_2) \implies T' = T_2 .$$

In words, T_2 is the unique minimizer of $\angle([T_1], \cdot)$ among triangles $T' \in \mathcal{F}(\mathcal{M})$ incident to E .

4.4 Intrinsic mesh inflation

In what follows, we consider an $(n - 1)$ -dimensional mesh \mathcal{M}_Γ with vertices in \mathbb{R}^n , where $n = 2$ or 3 . Let

$$\mathcal{F}_\Gamma := \{\text{oriented simplex of the form } [F] \text{ with } F \in \mathcal{M}_\Gamma\} . \quad (26)$$

Every element of \mathcal{M}_Γ appears twice in \mathcal{F}_Γ , once with each of the two opposite orientations.

Given $[F] \in \mathcal{F}_\Gamma$, and $S \in \mathcal{F}(F)$, let F' be the minimizer, among elements $F' \in \mathcal{M}_\Gamma$ incident to S (including F itself), of the quantity $\angle([F], F')$. Then define

$$\tilde{\mathcal{N}}_b([F], S) := [F']$$

where $[F']$ is the orientation of F' consistent with $[F]$.

Definition 12 (Intrinsic inflation). The *intrinsic inflation* of \mathcal{M}_Γ is the generalized mesh \mathcal{M}_Γ^* defined by

- the vertex set $\mathcal{V}_{\mathcal{M}_\Gamma^*} := \sigma_0(\mathcal{M}_\Gamma)$
- the elements $\mathbf{K}_{\mathcal{M}_\Gamma^*} := \mathcal{F}_\Gamma$,
- the realization $\mathcal{K}_{\mathcal{M}_\Gamma^*}$ defined by

$$\forall [F] \in \mathcal{F}_\Gamma, \quad \mathcal{K}_{\mathcal{M}_\Gamma^*}([F]) := F,$$

- the adjacency graph defined by

$$[F] \xleftrightarrow[\mathcal{M}_\Gamma^*]{S} [F'] \iff [F'] = \tilde{\mathcal{N}}_b([F], S)$$

By Lemma 10, and since an oriented triangle is never consistently oriented with itself, this is a well-defined generalized mesh.

Theorem 1. Let \mathcal{M}_Ω be a regular n -dimensional mesh in \mathbb{R}^n , with $n = 2$ or 3 , and let

$$\mathcal{M}_\Gamma \subset \mathcal{F}(\mathcal{M}_\Omega) \setminus \partial\mathcal{M}_\Omega.$$

Let $\mathcal{M}_\Gamma^*(\Omega)$ be the extrinsic inflation of \mathcal{M}_Γ via \mathcal{M}_Ω and \mathcal{M}_Γ^* the intrinsic inflation of \mathcal{M}_Γ , cf. Definitions 11 and 12 respectively. Then, $\mathcal{M}_\Gamma^*(\Omega)$ and \mathcal{M}_Γ^* are equal up to a relabeling.

Proof. To fix ideas, we write the proof for the case $n = 3$ (the case $n = 2$ is analogous). Recall that the elements of $\mathcal{M}_\Gamma^*(\Omega)$ are the pairs (F, K) with $K \in \mathcal{M}_\Omega$ and $F \in \mathcal{M}_\Gamma \cap \mathcal{F}(K)$. Given such a pair, we define

$$\varphi((F, K)) := [F]_{|[K]}$$

where $[K]$ is the natural orientation of K (recall the notation from Eq. (2)). Since \mathcal{M}_Γ is disjoint from the boundary of \mathcal{M}_Ω , by Lemma 2 this defines a bijection

$$\varphi : \mathbf{K}_{\mathcal{M}_\Gamma^*(\Omega)} \rightarrow \mathbf{K}_{\mathcal{M}_\Gamma^*},$$

with, obviously, $\mathcal{K}_1 \circ \varphi = \mathcal{K}_2$, where \mathcal{K}_1 and \mathcal{K}_2 are the realizations of \mathcal{M}_Γ^* and $\mathcal{M}_\Gamma^*(\Omega)$, respectively.

It remains to show that the adjacency graphs of \mathcal{M}_Γ^* and $\mathcal{M}_\Gamma^*(\Omega)$ are compatible with this bijection. This amounts to proving that, for $(F, K) \in \mathbf{K}_{\mathcal{M}_\Gamma^*(\Omega)}$ and $S \in \mathcal{F}(F)$, there holds

$$\varphi(\mathcal{N}_b((F, K), S)) = \tilde{\mathcal{N}}_b(\varphi((F, K)), S). \quad (27)$$

Hence, pick a pair $(F, K) \in \mathcal{M}_\Omega \times \mathcal{M}_\Gamma$, with $F \in \mathcal{F}(K)$, let $[F] = \varphi((F, K))$ and let $S \in \mathcal{F}(F)$. Let $\mathcal{M}_{\Omega \setminus \Gamma}^*$ be the fractured mesh defined by \mathcal{M}_Ω and \mathcal{M}_Γ (cf Definition 10). By definition of $\mathcal{M}_{\Omega \setminus \Gamma}^*$, we have

$$\perp \xleftrightarrow[\mathcal{M}_{\Omega \setminus \Gamma}^*]{F} K.$$

According to Lemma 6, we can introduce the chain

$$\perp \xleftrightarrow[\mathcal{M}_{\Omega \setminus \Gamma}^*]{F} K \xleftrightarrow[\mathcal{M}_{\Omega \setminus \Gamma}^*]{F_1} K_2 \xleftrightarrow[\mathcal{M}_{\Omega \setminus \Gamma}^*]{F_2} \dots \xleftrightarrow[\mathcal{M}_{\Omega \setminus \Gamma}^*]{F_{Q-2}} K_{Q-1} \xleftrightarrow[\mathcal{M}_{\Omega \setminus \Gamma}^*]{F_{Q-1}} K_Q \xleftrightarrow[\mathcal{M}_{\Omega \setminus \Gamma}^*]{F_Q} \perp. \quad (28)$$

Note that since $S \in \mathcal{F}(F_Q)$, $S \in \sigma(\mathcal{M}_\Gamma)$ and $\mathcal{M}_\Gamma \cap \partial\mathcal{M}_\Omega = \emptyset$, it must be true that $F_Q \in \mathcal{M}_\Gamma$. We rewrite $K' := K_Q$, $F' := F_Q$ so that

$$(F', K') = \mathcal{N}_b((F, K), S).$$

From Corollary 2, we deduce that for each $i \in \{1, \dots, Q\}$,

$$F_i = \arg \min \left\{ \angle([F], \tilde{F}) \mid \tilde{F} \in \mathcal{F}(\mathcal{M}_\Omega) \setminus \{F_j\}_{1 \leq j \leq i-1} \right\}.$$

By definition of $\mathcal{M}_{\Omega \setminus \Gamma}^*$, for $i \in \{1, \dots, Q-1\}$, the facet F_i is not in \mathcal{M}_Γ . Hence

$$F_Q = F' = \arg \min \left\{ \angle([F], \tilde{F}) \mid \tilde{F} \in \mathcal{M}_\Gamma \right\}. \quad (29)$$

Finally, let

$$[F'] := \varphi((F', K')).$$

Reasoning as in the proof of Lemma 9, we see that $[F]$ and $[F']$ are consistently oriented. From this property, Eq. (29) and Definition 12, it follows that

$$\tilde{\mathcal{N}}_b([F], S) = [F'],$$

which proves the claim (27) and concludes the proof of the theorem. \square

The following result is immediate, by the very definition of $\tilde{\mathcal{N}}_b$:

Lemma 12. *Let \mathcal{M}_Γ be a $(n-1)$ -dimensional generalized mesh in \mathbb{R}^n , with $n = 2$ or 3 . Then \mathcal{M}_Γ^* is orientable, with a compatible orientation given by*

$$\forall [F] \in \mathcal{M}_\Gamma^*, \quad [F]_{\mathcal{M}_\Gamma^*} := [F].$$

5 Finite element exterior calculus on generalized meshes

5.1 Whitney forms

We now fix the Euclidean space \mathbb{R}^m as the ambient space. Every generalized mesh discussed below has its vertices in \mathbb{R}^m and its elements are non-degenerate n -simplices, with $n \leq m$. Recall that for an element \mathbf{k} of \mathcal{M}^* attached to the simplex K , we write $|\mathbf{k}| := |K|$.

In this setting, we discuss the construction of lowest-order discrete differential forms on generalized meshes, which are the simplest specimen of trial and test spaces required for Finite-Element Exterior Calculus (FEEC, see [5]). Those spaces of discrete differential forms are spanned by locally supported basis functions, known as Whitney forms [31].

To define Whitney forms we need some additional structure. We have to choose an orientation for every simplex $S \in \sigma(\mathcal{M}^*)$. One standard way to do this is to choose an arbitrary order on the finite set $\sigma_0(\mathcal{M}^*)$ and equip each d -simplex $S = \{V_1, \dots, V_{d+1}\} \in \sigma_d(\mathcal{M}^*)$ with the orientation $[V_1, \dots, V_{d+1}]$. Typically, this doesn't incur any additional cost in the implementation, as simplices are stored using arrays, which are naturally ordered.

We also need *barycentric coordinate functions* on a non-degenerate n -simplex K . Given a vertex V of K , the barycentric coordinate $\lambda_V^K : \mathbb{R}^n \rightarrow \mathbb{R}$ is the affine function defined by the equations

$$\forall V' \in \sigma_0(K), \quad \lambda_V^K(V') = \begin{cases} 1 & \text{if } V = V', \\ 0 & \text{otherwise.} \end{cases} \quad (30)$$

Definition 13 (Whitney form associated to a generalized facet). Consider a generalized d -subfacet $\mathbf{s} \in \mathbf{S}_d(\mathcal{M}^*)$, $\mathbf{s} = (S, \gamma)$ with the orientation of S given by the order (V_1, \dots, V_{d+1}) . The associated *Whitney d -form* $\omega_{\mathbf{s}}$ is a tuple of differential forms

$$\omega_{\mathbf{s}} = (\omega_{\mathbf{s}}^{\mathbf{k}})_{\mathbf{k} \in \mathcal{M}^*}.$$

For each $\mathbf{k} \in \mathcal{M}^*$, $\omega_{\mathbf{s}}^{\mathbf{k}}$ is the d -differential form on $|\mathbf{k}|$ defined by

$$\omega_{\mathbf{s}}^{\mathbf{k}} := \begin{cases} \sum_{j=1}^{d+1} (-1)^{j+1} \lambda_{V_j}^K \wedge d\lambda_{V_1}^K \wedge \dots \wedge \widehat{d\lambda_{V_j}^K} \wedge \dots \wedge d\lambda_{V_{d+1}}^K, & \text{for } \mathbf{k} \in \gamma, \\ 0 & \text{for } \mathbf{k} \notin \gamma, \end{cases} \quad (31)$$

where K is the simplex attached to \mathbf{k} , d designates the exterior derivative, and the hat notation is used to denote a suppressed term.

It is a standard fact that this definition is correct, i.e. that the formula (31) is invariant with respect to even permutations of the chosen order (V_1, \dots, V_{d+1}) . Note that for $d = 0$, when S is a vertex, say V_1 , of K , then $\omega_{\mathbf{s}}^{\mathbf{k}}$ agrees with the barycentric coordinate function of K associated to the vertex V_1 when $\mathbf{k} \in \gamma$.

Using the vector space structure of tuples of differential forms, we can consider linear combinations of the Whitney forms defined above, and we define $\Lambda^d(\mathcal{M}^*)$ as the vector space spanned by $\{\omega_{\mathbf{s}}\}_{\mathbf{s} \in \mathbf{S}_d(\mathcal{M}^*)}$. We call its elements *Whitney d -forms on \mathcal{M}^** .

Definition 14 (Trace). Given a Whitney d -form $\omega = (\omega^{\mathbf{k}})_{\mathbf{k} \in \mathcal{M}^*} \in \Lambda^d(\mathcal{M}^*)$, the trace $\text{Tr} \omega$ is the Whitney d -form $\nu = (\nu^{\mathbf{f}})_{\mathbf{f} \in \partial \mathcal{M}^*} \in \Lambda^d(\partial \mathcal{M}^*)$ where, for each element $\mathbf{f} = (F, \mathbf{k})$ of $\partial \mathcal{M}^*$, $\nu^{\mathbf{f}}$ is given on $|F|$ by

$$\nu^{\mathbf{f}} := \text{Tr}_{|\mathbf{k}|, |F|} \omega^{\mathbf{k}}.$$

Here, $\text{Tr}_{\Omega, \Omega'} \mu$ is the *trace* of the differential form μ from the manifold Ω to the submanifold $\Omega' \subset \Omega$ [5, p.16]. It is defined as the pullback

$$\text{Tr}_{\Omega, \Omega'} \mu := \iota^* \mu$$

where ι is the inclusion $\Omega' \hookrightarrow \Omega$.

Lemma 13. *The Whitney d -forms satisfy the following patch condition: if $\mathbf{k} \xleftrightarrow[\mathcal{M}^*]{F} \mathbf{k}'$, then*

$$\forall \omega \in \Lambda^d(\mathcal{M}^*), \quad \text{Tr}_{|\mathbf{k}|, |F|} \omega^{\mathbf{k}} = \text{Tr}_{|\mathbf{k}'|, |F|} \omega^{\mathbf{k}'}$$

Proof. By linearity, it suffices to check that the patch condition is satisfied by $\omega_{\mathbf{s}}$ for each $\mathbf{s} \in \mathbf{S}_d(\mathcal{M}^*)$. Hence let $\mathbf{s} = (S, \gamma)$, with the orientation defined by the ordering (V_1, \dots, V_{d+1}) . We first remark that if K is the simplex attached to \mathbf{k} , and if $S \in \sigma(K)$ doesn't contain V_j , the function $\lambda_{V_j}^K$ is identically 0 on $|S|$. Hence, if F is a facet of \mathbf{k} not containing S , then $\omega_{\mathbf{s}}^{\mathbf{k}}$ vanishes on $|F|$. Consequently, if \mathbf{k} and \mathbf{k}' are adjacent through such a facet F , the patch condition is immediately verified. On the other hand, if F does contain S , then it follows that \mathbf{k} and \mathbf{k}' are adjacent through

S , so there are two cases: either $\mathbf{k} \notin \gamma$ and $\mathbf{k}' \notin \gamma$, either $\mathbf{k} \in \gamma$ and $\mathbf{k}' \in \gamma$. The patch condition is obvious in the former case since $\omega_{\mathbf{s}}$ then vanishes on both \mathbf{k} and \mathbf{k}' . Finally the patch condition in the latter case follows from

1. the property that if K is an n -simplex and F one of its facets, then

$$\forall V \in \sigma_0(F), \quad \lambda_V^F = \text{Tr}_{|K|,|F|} \lambda_V^K, \quad (32)$$

2. the commutation of pullbacks with wedge products and exterior derivative. \square

The significance of this lemma is to ensure that when \mathcal{M}^* is a fractured mesh, then $\Lambda^d(\mathcal{M}^*)$ is a subset of a suitable Sobolev space, see Section 6.2.

5.2 Surjectivity of the trace operator

In this section, we wish to identify a condition for Tr to be surjective from $\Lambda^d(\mathcal{M}^*)$ to $\Lambda^d(\partial\mathcal{M}^*)$. The importance of this surjectivity will be seen in Section 6.2. The main technical tool is given in the following lemma:

Lemma 14. *Let $\mathbf{s} = (S, \gamma) \in \mathbf{S}_d(\mathcal{M}^*)$ be a generalized d -subfacet of \mathcal{M}^* , and denote*

$$\text{st}_{\partial} \mathbf{s} := \{ \mathbf{f} = (F, \mathbf{k}) \in \partial\mathcal{M}^* \mid S \in \sigma(F) \text{ and } \mathbf{k} \in \gamma \}.$$

Assume that $\text{st}_{\partial} \mathbf{s}$ is non-empty and connected in \mathcal{M}^ , in the sense that for any two elements \mathbf{f}, \mathbf{f}' of $\text{st}_{\partial} \mathbf{s}$, there is a chain*

$$\mathbf{f} = \mathbf{f}_1 \xleftrightarrow[\partial\mathcal{M}^*]{S} \mathbf{f}_2 \xleftrightarrow[\partial\mathcal{M}^*]{S} \dots \xleftrightarrow[\partial\mathcal{M}^*]{S} \mathbf{f}_{Q-1} \xleftrightarrow[\partial\mathcal{M}^*]{S} \mathbf{f}_Q = \mathbf{f}',$$

with $\mathbf{f}_q \in \text{st}_{\partial} \mathbf{s}$ for each $q \in \{1, \dots, Q\}$. Then, there is a generalized d -subfacet \mathbf{t} of $\partial\mathcal{M}^$ given by $\mathbf{t} = (S, \text{st}_{\partial} \mathbf{s})$, and the Whitney forms $\omega_{\mathbf{s}} \in \Lambda^d(\mathcal{M}^*)$ and $\omega_{\mathbf{t}} \in \Lambda^d(\partial\mathcal{M}^*)$ are related by*

$$\text{Tr} \omega_{\mathbf{s}} = \pm \omega_{\mathbf{t}},$$

with a positive sign if the orientations of the simplex S in \mathcal{M}^ and $\partial\mathcal{M}^*$ agree, and negative otherwise.*

Proof. Pick an element $\mathbf{f}_0 = (F_0, \mathbf{k}_0) \in \text{st}_{\partial} \mathbf{s}$, and let $\mathbf{t} = (S, \eta) \in \mathbf{S}_d(\partial\mathcal{M}^*)$ be the unique generalized d -subfacet attached to S such that $\mathbf{f}_0 \in \eta$. We claim that

$$\eta = \text{st}_{\partial} \mathbf{s}. \quad (33)$$

Indeed, if \mathbf{f}' is another element of $\text{st}_{\partial} \mathbf{s}$, then by the assumption of the lemma, \mathbf{f}_0 and \mathbf{f}' are in the same component of the graph $\mathcal{G}_{\partial\mathcal{M}^*}(S)$, so $\mathbf{f}' \in \eta$. Hence $\text{st}_{\partial} \mathbf{s} \subset \eta$.

Conversely, if $\mathbf{f}' = (F', \mathbf{k}') \in \eta$, then \mathbf{f}' is in the same connected component as \mathbf{f}_0 in the graph $\mathcal{G}_{\partial\mathcal{M}^*}(S)$, which by definition of adjacency of the boundary, implies that \mathbf{k}' is in the same component as \mathbf{k}_0 in the graph $\mathcal{G}_{\mathcal{M}^*}(S)$. Hence $\mathbf{k}' \in \gamma$, so $\mathbf{f}' \in \text{st}_{\partial} \mathbf{s}$. Therefore, $\eta \subset \text{st}_{\partial} \mathbf{s}$, which proves (33).

Let $\mu = \text{Tr } \omega_{\mathbf{s}}$. For each $\mathbf{f} = (F, \mathbf{k}) \in \partial \mathcal{M}^*$, we compare the expressions of $\mu^{\mathbf{f}}$ and $\omega_{\mathbf{t}}^{\mathbf{f}}$. On the one hand, if $\mathbf{f} \in \text{st}_{\partial} \mathbf{s}$, then, writing $S = (V_1, \dots, V_{d+1})$ (with an order defining the orientation of S in \mathcal{M}^*), and denoting by K the simplex attached to \mathbf{k} ,

$$\begin{aligned} \mu^{\mathbf{f}} &= \text{Tr}_{|K|, |F|} \left(\sum_{j=1}^{d+1} (-1)^{j+1} \lambda_{V_j}^K \wedge d\lambda_{V_1}^K \dots \wedge \widehat{d\lambda_{V_j}^K} \wedge \dots \wedge d\lambda_{V_{d+1}}^K \right) \\ &= \sum_{j=1}^{d+1} (-1)^{j+1} \lambda_{V_j}^F \wedge d\lambda_{V_1}^F \dots \wedge \widehat{d\lambda_{V_j}^F} \wedge \dots \wedge d\lambda_{V_{d+1}}^F \end{aligned}$$

again by property (32). Clearly, this is equal to $\omega_{\mathbf{t}}^{\mathbf{f}}$ on $|F|$, up to a sign (the same sign will occur if the orientation of S in \mathcal{M}^* agrees with the one in $\partial \mathcal{M}^*$).

On the other hand, if $\mathbf{f} \notin \text{st}_{\partial} \mathbf{s}$, then $\omega_{\mathbf{t}}^{\mathbf{f}}$ vanishes on $|F|$, so it remains to check that the same holds for $\mu^{\mathbf{f}}$. By definition of $\text{st}_{\partial} \mathbf{s}$, either $\mathbf{k} \notin \gamma$, or $S \notin \sigma(F)$. In the former case, we have $\mu^{\mathbf{f}} = 0$ since $\omega_{\mathbf{s}}^{\mathbf{k}} = 0$. In the latter, there is a vertex V of S not in F , so $\lambda_V^K = 0$ identically on $|F|$. This confirms that $\mu^{\mathbf{f}}$ vanishes on $|F|$, and concludes the proof of the lemma. \square

Corollary 3. *Let \mathcal{M}^* be a generalized mesh such that for each d -simplex $S \in \sigma_d(\partial \mathcal{M}^*)$ and for each generalized d -subfacet $\mathbf{s} \in \mathbf{S}_d(\mathcal{M}^*)$ attached to S , $\text{st}_{\partial} \mathbf{s}$ satisfies the assumption of Lemma 14. Then, there holds*

$$\text{Tr}(\Lambda^d(\mathcal{M}^*)) = \Lambda^d(\partial \mathcal{M}^*).$$

Proof. Let $\mathbf{t} = (S, \eta) \in \mathbf{S}_d(\partial \mathcal{M}^*)$, pick $\mathbf{f}_0 = (F_0, \mathbf{k}_0) \in \eta$, and let $\mathbf{s} = (S, \gamma) \in \mathbf{S}_d(\mathcal{M}^*)$ be the generalized d -subfacet of \mathcal{M}^* defined by the condition that $\mathbf{k}_0 \in \gamma$. We have $\mathbf{f}_0 \in \text{st}_{\partial} \mathbf{s}$, so, following the beginning of the proof of Lemma 14, in fact $\mathbf{t} = (S, \text{st}_{\partial} \mathbf{s})$. Hence, by Lemma 14, there holds

$$\omega_{\mathbf{t}} = \pm \text{Tr } \omega_{\mathbf{s}}.$$

Since this holds for any $\mathbf{t} \in \mathbf{S}_d(\partial \mathcal{M}^*)$, the conclusion follows immediately. \square

The previous result has the following application in three dimensions: let \mathcal{M}_{Γ} be a triangular mesh and \mathcal{M}_{Ω} , a regular tetrahedral mesh such that $\mathcal{M}_{\Gamma} \subset \mathcal{F}(\mathcal{M}_{\Omega}) \setminus \partial \mathcal{M}_{\Omega}$. Correspondingly, let $\mathcal{M}_{\Omega \setminus \Gamma}^*$, $\mathcal{M}_{\Gamma}^*(\Omega)$ and \mathcal{M}_{Γ}^* be the fractured mesh (cf. Definition 10), the extrinsic inflation via \mathcal{M}_{Ω} (cf. Definition 11) and the intrinsic inflation of \mathcal{M}_{Γ} (cf. Definition 12), respectively. Since \mathcal{M}_{Γ}^* is a relabeling of $\mathcal{M}_{\Gamma}^*(\Omega)$ by Theorem 1, there exists a bijection

$$\varphi_{\Gamma} : \mathbf{K}_{\mathcal{M}_{\Gamma}^*} \rightarrow \mathbf{K}_{\mathcal{M}_{\Gamma}^*(\Omega)}$$

satisfying the conditions of Definition 3. Noting that $\mathbf{K}_{\mathcal{M}_{\Gamma}^*(\Omega)} \subset \mathbf{K}_{\partial \mathcal{M}_{\Omega \setminus \Gamma}^*}$, this allows to define a “pullback”

$$\begin{aligned} \varphi_{\Gamma}^* : \Lambda^d(\partial \mathcal{M}_{\Omega \setminus \Gamma}^*) &\rightarrow \Lambda^d(\mathcal{M}_{\Gamma}^*) \\ \omega &\mapsto \mu, \end{aligned}$$

where μ is defined by

$$\mu^{\mathbf{f}} := \omega^{\mathbf{f}'}, \quad \mathbf{f} \in \mathcal{M}_{\Gamma}^*, \quad \mathbf{f}' := \varphi_{\Gamma}(\mathbf{f}).$$

Essentially, φ_{Γ}^* is the restriction of Whitney d -forms from $\partial \mathcal{M}_{\Omega \setminus \Gamma}^*$ to \mathcal{M}_{Γ}^* .

Theorem 2. Assume that for each vertex S of \mathcal{M}_Γ , $\text{st}(S, \mathcal{M}_\Gamma)$ is edge-connected. Then the composition

$$\varphi_\Gamma^* \circ \text{Tr} : \Lambda^d(\mathcal{M}_{\Omega \setminus \Gamma}^*) \rightarrow \Lambda^d(\mathcal{M}_\Gamma^*)$$

is surjective. When $d = 0$, it is also necessary that $\text{st}(S, \mathcal{M}_\Gamma)$ be edge-connected for the surjectivity to hold.

The only challenging case is when $d = 0$. To avoid a lengthy proof, we limit ourselves to a rather informal description of the key idea. Given a vertex S of \mathcal{M}_Γ , one may look at $\mathcal{S} := \text{lk}(S, \mathcal{M}_\Omega)$, the link of S in \mathcal{M}_Ω , which is a triangular mesh homeomorphic to a sphere because \mathcal{M}_Ω is regular. On \mathcal{S} , some edges are incident to a triangle of \mathcal{M}_Γ : those edges define a plane graph G drawn on the surface of \mathcal{S} , as represented in Figure 12. Crucially, this graph is connected if and only if $\text{st}(S, \mathcal{M}_\Gamma)$ is edge-connected.

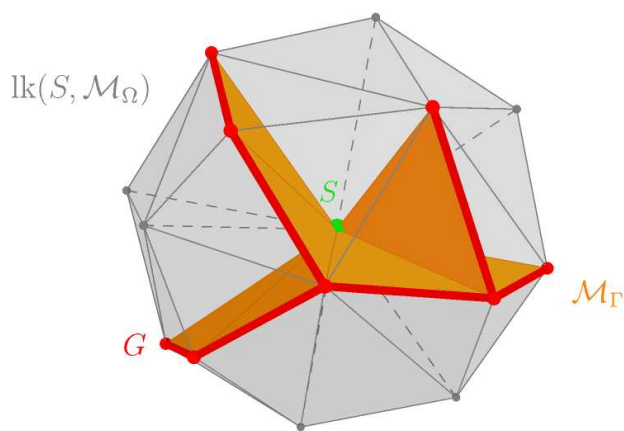


Figure 12: Illustration of the idea of the proof of Theorem 2. The link of the vertex S is represented in gray, the mesh \mathcal{M}_Γ in orange and the graph G drawn on $\text{lk}(S, \mathcal{M}_\Omega)$ in red.

To each generalized vertex $\mathbf{s} = (S, \gamma) \in \mathbf{S}_0(\mathcal{M}_{\Omega \setminus \Gamma}^*)$, corresponds a unique *face* f of G .⁴ Namely, if $\mathbf{k} \in \gamma$, K is the simplex attached to K , and F is the facet of K not containing S , then f is the face of G containing the interior of $|F|$. This correspondence is in fact bijective: each face of G corresponds to a unique generalized vertex attached to S .

To prove the lemma, the idea is then to show that $\text{st}_\partial \mathbf{s}$ is connected in the sense described in Lemma 14 if and only if the face f has a connected boundary.⁵ The conclusion follows from this and the observation that a plane graph is connected if and only if all of its faces have connected boundaries.

⁴A face of G is a connected component of $\mathcal{S} \setminus G$.

⁵In fact, the set $\text{st}_\partial \mathbf{s}$ is closely related to the set of edges visited by the “right-hand wall following” of G (in the “maze” whose walls are the edges of G , put a hand on a wall and keep walking forward, maintaining contact between your hand and the wall). The main task in the proof of Theorem 2 can be restated as follows: show that the right-hand wall following visits the connected component of the face boundary on which it starts.

5.3 Finite element assembly

Given an n -dimensional generalized mesh \mathcal{M}^* and $0 \leq d \leq n$, we discuss the computation of the Galerkin matrix associated to a bilinear form

$$a : \Lambda^d(\mathcal{M}^*) \times \Lambda^d(\mathcal{M}^*) \rightarrow \mathbb{R}.$$

We assume that a has the form

$$a(\omega, \omega') = \sum_{\mathbf{k} \in \mathcal{M}^*} a_{\mathbf{k}}(\omega_{\mathbf{k}}, \omega'_{\mathbf{k}}),$$

where for each $\mathbf{k} \in \mathcal{M}^*$, $a_{\mathbf{k}}$ is a bilinear form on the space of d -differential forms on $|\mathbf{k}|$. The Galerkin matrix \mathbf{A} of a is defined by

$$\mathbf{A}_{\mathbf{s}, \mathbf{t}} = a(\omega_{\mathbf{s}}, \omega_{\mathbf{t}}), \quad \mathbf{s}, \mathbf{t} \in \mathbf{S}_d(\mathcal{M}^*),$$

where $\{\omega_{\mathbf{s}}\}_{\mathbf{s} \in \mathbf{S}_d(\mathcal{M}^*)}$ is the Whitney form basis defined in the previous section. We use indexing by generalized d -subfacets to avoid the heavier notation that would result from introducing orderings.

As in standard finite element computations, one first needs a method to compute so-called *local matrices*, involving the local Whitney forms defined on each element. For each d -subsimplex S of an element $\mathbf{k} \in \mathcal{M}^*$, there is a unique generalized q -subfacet \mathbf{s} of the form

$$\mathbf{s} = (S, \gamma) \text{ with } \mathbf{k} \in \gamma.$$

We write $\mathbf{s} =: J(\mathbf{k}, S)$. In the implementation, J corresponds to a “local-to-global” index mapping. One can then form the local $\binom{n}{d} \times \binom{n}{d}$ matrices $A_{loc}(\mathbf{k})$, defined by

$$[A_{loc}(\mathbf{k})]_{S, S'} := a(\omega_{\mathbf{s}}^{\mathbf{k}}, \omega_{\mathbf{s}'}^{\mathbf{k}}) \quad S, S' \in \sigma_d(\mathbf{k}), \mathbf{s} = J(\mathbf{k}, S), \mathbf{s}' = J(\mathbf{k}, S').$$

To assemble the global matrix \mathbf{A} from the local matrices A_{loc} , one can then use Algorithm 3 below:

Algorithm 3 Assembly($\mathcal{M}^*, d, A_{loc}$)

INPUTS: Generalized mesh \mathcal{M}^* , subsimplex dimension d , local matrices A_{loc}

RETURNS: The (sparse) matrix \mathbf{A} .

$N_d \leftarrow \text{Card}(\mathbf{S}_d(\mathcal{M}^*))$ % Number of generalized d -subfacets

$\mathbf{A} \leftarrow \text{zeros}(N_d, N_d)$ % Initialize matrix

FOR $\mathbf{k} \in \mathbf{K}_{\mathcal{M}^*}$

$A \leftarrow A_{loc}(\mathbf{k})$ % Compute local matrix

FOR $S, S' \in \sigma_d(\mathbf{k})$

$\mathbf{s} \leftarrow J(\mathbf{k}, S)$ % find indices in global matrix

$\mathbf{t} \leftarrow J(\mathbf{k}, S')$

$\mathbf{A}_{\mathbf{s}, \mathbf{t}} \leftarrow \mathbf{A}_{\mathbf{s}, \mathbf{t}} + A(S, S')$ % add local contribution to the global matrix

END FOR

END FOR

RETURN \mathbf{A}

In the context of boundary elements, the bilinear form a rather takes the form

$$a(\omega, \omega') = \sum_{\mathbf{k} \in \mathbf{K}_{\mathcal{M}^*}} \sum_{\mathbf{k}' \in \mathbf{K}_{\mathcal{M}^*}} a_{\mathbf{k}, \mathbf{k}'}(\omega_{\mathbf{k}}, \omega'_{\mathbf{k}'}).$$

This case can be tackled very similarly, using two nested loops over elements, instead of just one, in Algorithm 3.

6 Numerical experiments

To conclude this paper, we present two applications of generalized meshes to the resolution of PDEs in non regular geometries.

6.1 Laplace eigenvalue problem in a disk with cut radius

First, we solve the Laplace equation in a disk with cut radius, i.e. the domain

$$\Omega = B(0, 1) \setminus ([0, 1] \times \{0\}) \subset \mathbb{R}^2.$$

Generalized meshes are perfectly suited to represent such a geometry, see e.g. Figure 13 below. To create meshes like this one, we have implemented a function

$$\mathcal{M}_{\Omega \setminus \Gamma}^* = \text{fracturedMesh}(\mathcal{M}_{\Omega}, \mathcal{M}_{\Gamma})$$

which takes as an input a regular n -dimensional mesh \mathcal{M}_{Ω} , a $(n-1)$ -dimensional mesh \mathcal{M}_{Γ} such that $\mathcal{M}_{\Gamma} \subset \mathcal{F}(\mathcal{M}_{\Omega})$, and returns the fractured mesh $\mathcal{M}_{\Omega \setminus \Gamma}^*$ as defined in Section 4. Then, the Galerkin matrices in the basis $\{\omega_{\mathbf{v}}\}_{\mathbf{v} \in \mathbf{S}_0(\mathcal{M}_{\Omega \setminus \Gamma}^*)}$ of the operators needed, (i.e. the mass matrix, for the identity operator, and the stiffness matrix, for the Laplace operator) can be assembled by using Algorithm 3.⁶

If initially, the mesh \mathcal{M}_{Ω} does not resolve the fracture, in the sense that $\mathcal{M}_{\Gamma} \subset \mathcal{F}(\mathcal{M}_{\Omega})$ is not fulfilled, then one may remesh the domain \mathcal{M}_{Ω} using constrained meshing algorithms, see e.g. [10].

The eigenvalue problem reads formally

$$\begin{cases} \Delta u = \lambda u & \text{in } \Omega, \\ \partial_n u = 0 & \text{on } \partial\Omega, \end{cases} \quad (34)$$

and its solutions can be found analytically by separation of variables; they take the form

$$u_{n,p}(r, \theta) = f_p(r)g_n(\theta)$$

with

$$\begin{aligned} g_n(\theta) &= \cos(n\theta/2), \quad n \in \mathbb{N}, \\ f_p(r) &= J_{\frac{n}{2}}(\rho_{n,p}r), \quad p \in \mathbb{N}, \end{aligned}$$

where $\rho_{n,p}$ is the p -th zero of $J'_{n/2}$. The associated eigenvalue is $\lambda_{n,p} = \rho_{n,p}^2$.

⁶For our Matlab implementation, we have rather adopted a global assembly algorithm as in [3], in which the nested loops can be avoided to increase the performance.

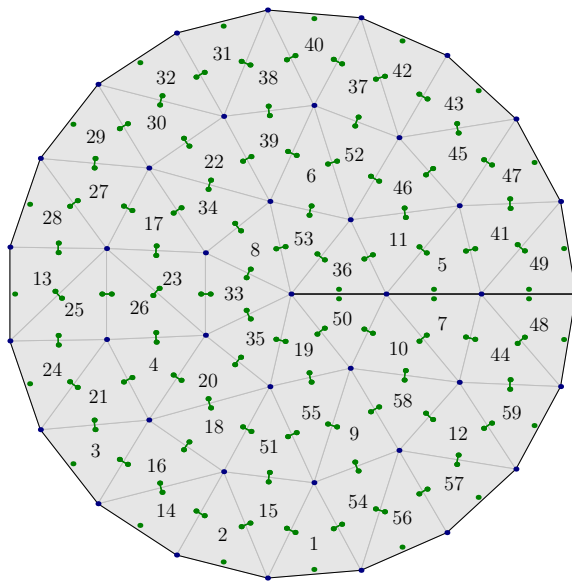


Figure 13: Generalized mesh representing a disk with cut radius. The adjacency graph is represented in green, with the same conventions as in Figures 3 and 6

To test our implementation, we compute numerical approximations of those eigenvalues using a variational formulation and the finite element method on a generalized mesh like the one of Figure 13. We do not dwell on the details of the method, but refer to our Matlab implementation. The numerical values of the first $\lambda_{n,p}$ that we obtain for various mesh sizes are compared against reference values computed to high precision using a Newton iteration. The numerical values indeed approach the reference values, see Table 1. The fact that the first non-constant eigenfunction,

$$u_{1,1}(r, \theta) = J_{1/2}(\sqrt{\lambda_{1,1}}r) \cos(\theta/2)$$

behaves like $O(\sqrt{r})$ near the origin, explains the slow rate of convergence for the corresponding eigenvalue, and is a manifestation of a well-known feature in the field of fracture physics (see e.g. [25, Chap.3]), the so-called “crack-tip singularity”.

One can of course tackle more complex geometries and PDEs, use vectorial elements and work in three dimensions. Here we have restricted our attention to the simplest model problem for the sake of clarity.

6.2 Laplace hypersingular equation on a multi-screen

Introduction

To conclude this paper, we consider the resolution of a Laplace hypersingular integral equation on a multi-screen. This is the main intended application of this work.

Multi-screens were introduced by two of the authors in [18] as a model for complex geometries that fall out of the scope of orientable Lipschitz manifolds. A representative example of a multi-screen is the geometry depicted in Figure 1. Many linear PDEs in the domain surrounding a

	$h \approx 0.7$	$h \approx 0.35$	$h \approx 0.18$	$h \approx 0.09$
$ \lambda_{1,h} - \lambda_1 /\lambda_1$	0.15152	0.062438	0.028606	0.014625
$ \lambda_{2,h} - \lambda_2 /\lambda_2$	0.046833	0.01163	0.0028283	0.00083173
$ \lambda_{3,h} - \lambda_3 /\lambda_3$	0.054236	0.015154	0.0039806	0.0011769
$ \lambda_{4,h} - \lambda_4 /\lambda_4$	0.076291	0.021513	0.0057585	0.0016574
$ \lambda_{5,h} - \lambda_5 /\lambda_5$	0.094939	0.028421	0.007837	0.002246

Table 1: Numerical approximations of the the first eigenvalues of the Neumann eigenvalue problem on the disk with cut radius as computed by the finite element method, compared to theoretical value. We report the relative error $|\lambda_{i,h} - \lambda_i|/\lambda_i$ where $\lambda_{i,h}$ is the numerical approximation returned by the finite element method and λ_i is the corresponding reference value. The parameter h is the diameter of the smallest element in the mesh. The first eigenvalue, $\lambda_0 = 0$, is ignored.

multi-screen can be recast as boundary integral equations on the surface of the multi-screen, but this requires the introduction of adapted Sobolev trace spaces for such singular geometry. We will summarize the essential aspects below, and refer to [18] for the details.

A fist work on the numerical implementation of this method has been published [19]. We will now revisit more formally some parts of that previous article:

- As we have already seen, the intrinsic inflation method, described in Section 4.4 provides a generic algorithm to create the “inflated mesh” associated to a multi-screen [19, Section 4.1],
- The concepts of Section 5 will allow for a more formal description of the spaces introduced in [19, Section 4.2],
- Theorem 1 allows for a characterization of the space of Whitney forms on the multi-screen as the range of the multi-trace operator applied to Whitney forms in the volume surrounding the multi-screen (see Lemma 15),
- Finally, the notion of generalized subfacets allows to get rid of the kernel of the linear systems to be eventually solved, making it unnecessary to work with quotient-space iterative methods.

Abstract Galerkin method

We consider a triangular mesh \mathcal{M}_Γ in \mathbb{R}^3 , and assume that

$$|\mathcal{M}_\Gamma| = \Gamma$$

where Γ is a multi-screen. This means [18, Definition 2.3] that there are disjoint Lipschitz domains $\Omega_1, \dots, \Omega_J$ such that

- $\mathbb{R}^3 = \bigcup_{j=1}^J \bar{\Omega}_j$
- $\Gamma \subset \bigcup_{j=1}^J \partial\Omega_j$
- For each $1 \leq j \leq J$, $\Gamma_j := \bar{\Gamma} \cap \partial\Omega_j$ is a Lipschitz screen in the sense of [15, Section 1.1].

We also assume that Γ and $\mathbb{R}^3 \setminus \bar{\Gamma}$ are connected and further that \mathcal{M}_Γ satisfies the following property:

$$\forall S \in \sigma(\mathcal{M}_\Gamma), \quad \text{st}(S, \mathcal{M}_\Gamma) \text{ is edge-connected.} \quad (35)$$

An example of such mesh is given by Figure 1. The condition above rules out “point contacts” between triangles, as in Figure 14 below.

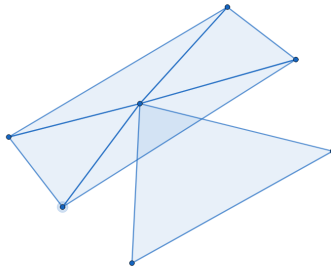


Figure 14: A mesh that does not satisfy condition (35).

Condition (35) might be automatically implied by the fact that $|\mathcal{M}_\Gamma|$ is a multi-screen, but we shall not attempt to prove this implication.

Recall from [18, Section 4] the definitions of the spaces $\mathbb{H}^1(\mathbb{R}^3 \setminus \bar{\Gamma})$, $\mathbb{H}(\text{div}, \mathbb{R}^3 \setminus \bar{\Gamma})$, $\mathbb{H}_{0,\Gamma}^1(\mathbb{R}^3)$ and $\mathbb{H}_{0,\Gamma}(\text{div}, \mathbb{R}^3)$. The *multi-trace* spaces are the quotient spaces

$$\mathbb{H}^{1/2}(\Gamma) = \mathbb{H}^1(\mathbb{R}^3 \setminus \bar{\Gamma}) / \mathbb{H}_{0,\Gamma}^1(\mathbb{R}^3), \quad \mathbb{H}^{-1/2}(\Gamma) = \mathbb{H}(\text{div}, \mathbb{R}^3 \setminus \bar{\Gamma}) / \mathbb{H}_{0,\Gamma}(\text{div}, \mathbb{R}^3).$$

By π_D and π_N we denote the associated canonical surjections. Let the bilinear form $\langle\langle \cdot, \cdot \rangle\rangle : \mathbb{H}^{1/2}(\Gamma) \times \mathbb{H}^{-1/2}(\Gamma) \rightarrow \mathbb{C}$ be defined by

$$\langle\langle \dot{u}, \dot{\mathbf{p}} \rangle\rangle := \int_{\mathbb{R}^d \setminus \bar{\Gamma}} \mathbf{p} \cdot \nabla u + u \text{div}(\mathbf{p}) \, dx$$

where $\pi_D(u) = \dot{u}$ and $\pi_N(\mathbf{p}) = \dot{\mathbf{p}}$ (the value of the rhs does not depend on the choice of the representatives) [18, Prop. 5.1]. The *single-trace* spaces are the closed subspaces of the respective multi-trace spaces defined by

$$\mathbb{H}^{1/2}([\Gamma]) := \pi_D(\mathbb{H}^1(\mathbb{R}^3)), \quad \mathbb{H}^{-1/2}([\Gamma]) := \pi_N(\mathbb{H}(\text{div}, \mathbb{R}^3)).$$

The *jump spaces* are defined as the duals

$$\tilde{\mathbb{H}}^{\pm 1/2}([\Gamma]) := (\mathbb{H}^{\mp 1/2}([\Gamma]))',$$

and one can define two continuous and surjective *jump operators* (denoted in the same way): $[\cdot] : \mathbb{H}^{\pm 1/2}(\Gamma) \rightarrow \tilde{\mathbb{H}}^{\pm 1/2}([\Gamma])$ by

$$\begin{aligned} \langle [\dot{u}], \dot{\mathbf{p}} \rangle &:= \langle\langle \dot{u}, \dot{\mathbf{p}} \rangle\rangle, \quad (\dot{u}, \dot{\mathbf{p}}) \in \mathbb{H}^{1/2}([\Gamma]) \times \mathbb{H}^{-1/2}([\Gamma]) \\ \langle [\dot{\mathbf{p}}], \dot{u} \rangle &:= \langle\langle \dot{u}, \dot{\mathbf{p}} \rangle\rangle, \quad (\dot{u}, \dot{\mathbf{p}}) \in \mathbb{H}^{1/2}([\Gamma]) \times \mathbb{H}^{-1/2}(\Gamma), \end{aligned}$$

which furthermore satisfy (see [18, Props. 6.3])

$$\begin{aligned}\forall \dot{u} \in \mathbb{H}^{1/2}(\Gamma), \quad [\dot{u}] = 0 &\iff \dot{u} \in \mathbf{H}^{1/2}([\Gamma]), \\ \forall \dot{\boldsymbol{p}} \in \mathbb{H}^{-1/2}(\Gamma), \quad [\dot{\boldsymbol{p}}] = 0 &\iff \dot{\boldsymbol{p}} \in \mathbf{H}^{-1/2}([\Gamma]),\end{aligned}$$

A double-layer potential $\text{DL} : \mathbb{H}^{1/2}(\Gamma) \rightarrow C^\infty(\mathbb{R}^3 \setminus \bar{\Gamma})$ can be defined [18, Section 8]. When solving the following Neumann boundary value problem:

$$\begin{cases} \Delta H &= 0 & \text{on } \mathbb{R}^d \setminus \bar{\Gamma}, \\ \pi_N(\nabla H) &= \dot{\boldsymbol{g}} & \text{on } \Gamma, \\ H(\boldsymbol{x}) &\rightarrow 0 & \boldsymbol{x} \rightarrow \infty, \end{cases} \quad (36)$$

with $\dot{\boldsymbol{g}} \in \mathbf{H}^{-1/2}([\Gamma])$, one can seek a solution in the form

$$H = \text{DL } \dot{u}.$$

A necessary and sufficient condition for this ansatz to solve problem (36) is that \dot{u} solve the variational problem

$$a(\dot{u}, \dot{v}) = \langle \dot{v}, \dot{\boldsymbol{g}} \rangle, \quad \forall \dot{v} \in \mathbb{H}^{1/2}(\Gamma), \quad (37)$$

where the bilinear form $a : \mathbb{H}^{1/2}(\Gamma) \times \mathbb{H}^{1/2}(\Gamma)$ is defined by

$$a(\dot{u}, \dot{v}) = \langle \dot{v}, \pi_N(\nabla \text{DL } \dot{u}) \rangle.$$

However, because of the property

$$\forall \dot{u} \in \mathbf{H}^{1/2}([\Gamma]), \quad [\pi_N(\nabla \text{DL } \dot{u})] = 0$$

it follows that, whenever $\dot{u} \in \mathbf{H}^{1/2}([\Gamma])$ or $\dot{v} \in \mathbf{H}^{1/2}([\Gamma])$, $a(\dot{u}, \dot{v}) = 0$. Hence the variational problem (37) is not uniquely solvable, and this is the reason why the authors of [19] used quotient-space iterative methods. Nevertheless, one can define an other bilinear form $\tilde{a} : \tilde{\mathbf{H}}^{1/2}([\Gamma]) \times \tilde{\mathbf{H}}^{1/2}([\Gamma]) \rightarrow \mathbb{R}$ by

$$\tilde{a}(\tilde{u}, \tilde{v}) := a(\dot{u}, \dot{v})$$

whenever $[\dot{u}] = \tilde{u}$ and $[\dot{v}] = \tilde{v}$. This definition is independent of the choice of \dot{u} and \dot{v} satisfying this condition. Moreover, \dot{u} solves the variational problem (37) if and only if $\tilde{u} = [\dot{u}]$ solves the new variational problem

$$\tilde{a}(\tilde{u}, \tilde{v}) = \langle \tilde{v}, \dot{\boldsymbol{g}} \rangle, \quad \forall \tilde{v} \in \tilde{\mathbf{H}}^{-1/2}([\Gamma]). \quad (38)$$

One can show that \tilde{a} is positive definite [7], and as a consequence of [18, Prop. 8.9], there exists a constant $c > 0$ such that

$$\forall \tilde{u} \in \tilde{\mathbf{H}}^{1/2}([\Gamma]), \quad \tilde{a}(\tilde{u}, \tilde{u}) \geq c \|\tilde{u}\|_{\tilde{\mathbf{H}}^{1/2}([\Gamma])}^2. \quad (39)$$

Hence, according to standard Galerkin theory, given a sequence of spaces $\tilde{V}_n \subset \tilde{\mathbf{H}}^{1/2}([\Gamma])$, one can compute a sequence of approximations \tilde{u}_n of the solution \tilde{u} of (38), which converge (quasi-optimally) to \tilde{u} in $\tilde{\mathbf{H}}^{1/2}([\Gamma])$ provided that

$$\forall \tilde{v} \in \tilde{\mathbf{H}}^{1/2}([\Gamma]), \quad \lim_{n \rightarrow \infty} \sup_{\tilde{w} \in \tilde{V}_n} \|\tilde{v} - \tilde{w}\|_{\tilde{\mathbf{H}}^{1/2}([\Gamma])} = 0. \quad (40)$$

Construction of the discrete spaces

We construct the spaces \tilde{V}_n as follows. We start by considering a Lipschitz domain Ω surrounding Γ and a Lipschitz partition $\Omega_0, \Omega_1, \dots, \Omega_J$ of disjoint Lipschitz domains such that

$$\mathbb{R}^3 = \bigcup_{j=0}^J \bar{\Omega}_j$$

with $\Omega_0 = \mathbb{R}^3 \setminus \bar{\Omega}$. Let $\mathcal{M}_{\Omega_1}, \dots, \mathcal{M}_{\Omega_J}$ be regular tetrahedral meshes such that

- $|\mathcal{M}_{\Omega_j}| = \Omega_j$
- $\mathcal{M}_{\Omega} := \bigcup_{j=1}^J \mathcal{M}_{\Omega_j}$ is a regular mesh and $|\mathcal{M}_{\Omega}| = \Omega$.
- $\mathcal{M}_{\Gamma} \subset \mathcal{F}(\mathcal{M}_{\Omega}) \setminus \partial\mathcal{M}_{\Omega}$.

For each $h > 0$, we assume the existence of refinements⁷ $\mathcal{M}_{\Omega_j, h}$ (resp. $\mathcal{M}_{\Omega, h}, \mathcal{M}_{\Gamma, h}$) of \mathcal{M}_{Ω_j} (resp. $\mathcal{M}_{\Omega}, \mathcal{M}_{\Gamma}$) whose element diameters do not exceed h , and such that the family of meshes $(\mathcal{M}_{\Omega_j, h})_{h>0}$ (resp. $(\mathcal{M}_{\Omega, h})_{h>0}, (\mathcal{M}_{\Gamma, h})_{h>0}$) be shape-regular [21, Def. 1.107] and $\mathcal{M}_{\Gamma, h} \subset \mathcal{F}(\mathcal{M}_{\Omega, h})$. This can be achieved for example using tetrahedral refinement methods, see e.g. [27]. For each $h > 0$, we define

$$V_h(\Omega \setminus \bar{\Gamma}) := \left\{ u \in \Lambda^0(\mathcal{M}_{\Omega \setminus \Gamma, h}^*) \mid u = 0 \text{ on } \partial\Omega \right\}$$

where $\mathcal{M}_{\Omega \setminus \Gamma, h}^*$ is the fractured mesh defined by \mathcal{M}_{Ω}^h and \mathcal{M}_{Γ}^h and $\Lambda^0(\mathcal{M}^*)$ is the set of 0-Whitney forms as defined in Section 5. Thanks to the patch condition established in Lemma 13, we can view $V_h(\Omega \setminus \bar{\Gamma})$ as a subspace of $H^1(\mathbb{R}^3 \setminus \bar{\Gamma})$. Intuitively, $V_h(\Omega \setminus \bar{\Gamma})$ is a space of Lagrange piecewise linear functions on the mesh \mathcal{M}_{Ω} , that are allowed to “jump” across Γ .

Next, we define

$$\mathbb{V}_h(\Gamma) := \pi_D(V_h(\Omega \setminus \bar{\Gamma})), \quad V_h([\Gamma]) := \pi_D(C^0(\mathbb{R}^3) \cap V_h(\Omega \setminus \bar{\Gamma})), \quad \tilde{V}_h([\Gamma]) := [V_h([\Gamma])].$$

It follows immediately from these definitions that

$$\mathbb{V}_h(\Gamma) \subset \mathbb{H}^{1/2}(\Gamma), \quad V_h([\Gamma]) \subset H^{1/2}([\Gamma]), \quad \tilde{V}_h(\Gamma) \subset \tilde{H}^{1/2}([\Gamma]),$$

and hence $\tilde{V}_h(\Gamma)$ is a candidate to play the role of the subspace \tilde{V}_n . The approximation property (40) follows from approximation properties of the spaces $V_h(\Omega \setminus \bar{\Gamma})$ in a subspace of $H^1(\mathbb{R}^3 \setminus \bar{\Gamma})$ and the continuity of the operator π_D . We refer to [8] for quantitative results on this topic.

In the next lemma, we further characterize $\mathbb{V}_h(\Gamma)$ and state an important formula for the bilinear form a :

Lemma 15 (Characterization of $\mathbb{V}_h(\Gamma)$). *One has an isomorphism*

$$\mathcal{J}_h : \mathbb{V}_h(\Gamma) \simeq \Lambda^0(\mathcal{M}_{\Gamma, h}^*),$$

where $\mathcal{M}_{\Gamma, h}^*$ is the virtual inflation of \mathcal{M}_{Γ}^h . Moreover, there holds

$$a(u, v) = \sum_{\mathbf{k} \in \mathcal{M}_{\Gamma, h}^*} \sum_{\mathbf{k}' \in \mathcal{M}_{\Gamma, h}^*} a_{\mathbf{k}, \mathbf{k}'}(\omega_{\mathbf{k}}, \omega'_{\mathbf{k}'}), \quad u, v \in \mathbb{V}_h(\Gamma) \quad (41)$$

⁷A mesh \mathcal{M}_2 is a refinement of \mathcal{M}_1 if $|\mathcal{M}_1| = |\mathcal{M}_2|$ and for each element $K \in \mathcal{M}_1$, there is a subset $m_2 \subset \mathcal{M}_2$ such that m_2 is a regular mesh and $|m_2| = |K|$.

where $\omega = \mathcal{J}_h u$, $\omega' = \mathcal{J}_h v$, and

$$a_{\mathbf{k}, \mathbf{k}'}(\omega_{\mathbf{k}}, \omega'_{\mathbf{k}'}) = \int_{|\mathbf{k}| \times |\mathbf{k}'|} \frac{\langle \delta \omega_{\mathbf{k}}(x), \delta \omega'_{\mathbf{k}'}(y) \rangle}{4\pi \|x - y\|} dx dy. \quad (42)$$

where the operator δ and the inner product $\langle \cdot, \cdot \rangle$ are defined in [5].

Proof. By Theorem 2, the operator $\varphi_{\Gamma}^* \circ \text{Tr}$ maps surjectively

$$\varphi_{\Gamma}^* \circ \text{Tr} : V_h(\Omega \setminus \bar{\Gamma}) \rightarrow \Lambda^0(\mathcal{M}_{\Gamma, h}^*).$$

To proceed, we use the following property: a function $u \in \mathbf{H}^1(\mathbb{R}^3 \setminus \bar{\Gamma})$ is such that for all $j = 1 \dots J$, the trace $\gamma(u|_{\Omega_j})$ vanishes on Γ_j , if and only if $u \in \mathbf{H}_{0, \Gamma}^1(\mathbb{R}^3)$ (this result can be found e.g. in [8]). We deduce that

$$\text{Ker}(\varphi_{\Gamma}^* \circ \text{Tr}) = V_h(\Omega \setminus \bar{\Gamma}) \cap \mathbf{H}_{0, \Gamma}^1(\mathbb{R}^3)$$

and thus $\varphi_{\Gamma}^* \circ \text{Tr}$ induces an isomorphism on the quotient space:

$$\mathcal{J}_h : \mathbb{V}_h(\Gamma) \rightarrow \Lambda^0(\mathcal{M}_{\Gamma, h}^*).$$

Finally, we prove eqs. (41) and (42) in [7] (those formulas are also stated in [19]). \square

Remark 2. Note that if $\omega_{\mathbf{k}}$ is regarded as a scalar linear function on $|\mathbf{k}|$, then one can rewrite Eq. (42) in the more familiar form

$$a_{\mathbf{k}, \mathbf{k}'}(\omega_{\mathbf{k}}, \omega'_{\mathbf{k}'}) = \int_{|\mathbf{k}| \times |\mathbf{k}'|} \frac{\mathbf{curl} \omega_{\mathbf{k}}(x) \cdot \mathbf{curl} \omega'_{\mathbf{k}'}(y)}{4\pi \|x - y\|} dx dy.$$

From now on, we omit the isomorphism \mathcal{J}_h and identify $\mathbb{V}_h(\Gamma)$ to $\Lambda^0(\mathcal{M}_{\Gamma, h}^*)$. Now, we turn our attention to the space $\tilde{V}_h(\Gamma)$. Let $Y_h([\Gamma])$ be a complement of $V_h([\Gamma])$ in $\mathbb{V}_h(\Gamma)$, i.e.

$$\mathbb{V}_h(\Gamma) = V_h([\Gamma]) \oplus Y_h([\Gamma]).$$

We denote by \tilde{N}_h the dimension of $Y_h(\Gamma)$. Then, the jump operator maps

$$[\cdot] : Y_h([\Gamma]) \rightarrow \tilde{V}_h(\Gamma)$$

bijectively. In particular, given $\{e_i\}_{1 \leq i \leq \tilde{N}_h}$ a basis of $Y_h([\Gamma])$, the family $\{\tilde{e}_i\}_{1 \leq i \leq \tilde{N}_h}$ is a basis of $\tilde{V}_h([\Gamma])$, with $\tilde{e}_i := [e_i]$. Moreover, if P is the rectangular matrix defined by

$$e_i = \sum_{\mathbf{v} \in \mathbf{S}_0(\mathcal{M}_{\Gamma, h}^*)} P_{i, \mathbf{v}} \omega_{\mathbf{v}}, \quad 1 \leq i \leq \tilde{N}_h,$$

then there holds

$$\tilde{W} = PWP',$$

where W (resp. \tilde{W}) is the matrix of the bilinear forms a (resp. \tilde{a}) in the basis $\{\omega_{\mathbf{v}}\}_{\mathbf{v} \in \mathbf{S}_0(\mathcal{M}_{\Gamma, h}^*)}$ (resp. $\{\tilde{e}_i\}_{1 \leq i \leq \tilde{N}_h}$).

It remains to propose a candidate for the space $Y_h([\Gamma])$, and its basis. We start by a simple characterization of $V_h([\Gamma])$.

Lemma 16 (Characterization of $V_h([\Gamma])$). $V_h([\Gamma])$ is (isomorphic to) the vector subspace of $\Lambda^0(\mathcal{M}_{\Gamma,h}^*)$ spanned by the forms

$$\omega_V := \sum_{\mathbf{v}} \omega_{\mathbf{v}},$$

where $V \in \sigma_0(\mathcal{M}_{\Gamma,h}^*)$ is a vertex of $\mathcal{M}_{\Gamma,h}^*$ and the sum extends over all generalized vertices $\mathbf{v} \in \mathbf{S}_0(\mathcal{M}_{\Gamma,h}^*)$ attached to V .

Proof. Let $\dot{u} \in V_h([\Gamma])$ and let $u \in C^0(\mathbb{R}^3) \cap V_h(\Omega \setminus \bar{\Gamma})$ be a representative of \dot{u} . This is nothing else than a piecewise linear continuous function on the mesh \mathcal{M}_Ω , so we have

$$u = \sum_{V \in \sigma_0(\mathcal{M}_\Omega)} u(V) \lambda_V$$

where λ_V is the “tent function” associated to the vertex V in the mesh \mathcal{M}_Ω . Hence

$$\varphi_\Gamma^* \circ \text{Tr } u = \sum_{V \in \sigma_0(\mathcal{M}_\Omega)} u(V) \varphi_\Gamma^* \circ \text{Tr}(\lambda_V).$$

Finally, one can check that

$$\varphi_\Gamma^* \circ \text{Tr}(\lambda_V) = \sum_{\mathbf{v}} \omega_{\mathbf{v}}$$

where the sum extends over all generalized vertices $\mathbf{v} \in \mathbf{S}_0(\mathcal{M}_{\Gamma,h}^*)$ attached to V , by examining the definition of Tr and φ_Γ^* . This concludes the proof. \square

We now define $Y_h([\Gamma])$ directly by specifying its basis $\{e_i\}_{1 \leq i \leq \tilde{N}_h}$. For each vertex $V \in \sigma_0(\mathcal{M}_{\Gamma,h}^*)$, we consider the set of $\{\mathbf{v}_1, \dots, \mathbf{v}_L\}$ of generalized vertices attached to V . For $l = 1 \dots L - 1$, let

$$e_{V,l} := \omega_{\mathbf{v}_l} - \omega_{\mathbf{v}_L}.$$

We define $\{e_i\}_{1 \leq i \leq \tilde{N}_h}$ as the set of all functions obtained in this way. Clearly, the subspace $Y_h([\Gamma])$ that they span is a complement of $V_h([\Gamma])$ in $\mathbb{V}_h(\Gamma)$.

Results

For the concrete application, we consider the following triangular mesh

$$\mathcal{M}_\Gamma = \{\text{OIJ}, \text{OI}'\text{J}, \text{OIJ}', \text{OI}'\text{J}', \text{OIK}, \text{OJK}, \text{OI}'\text{K}, \text{OJ}'\text{K}, \text{OIK}', \text{OJK}', \text{OI}'\text{K}'\}.$$

where

$$\text{O} = (0, 0, 0), \quad \text{I} = (1, 0, 0), \quad \text{J} = (0, 1, 0), \quad \text{K} = (0, 0, 1),$$

and $\text{I}' = -\text{I}, \text{J}' = -\text{J}, \text{K}' = -\text{K}$. A 3D representation of \mathcal{M}_Γ is given in Figure 15. To avoid some symmetries and to have more varied generalized vertices, we intentionally omit the triangle $\text{OJ}'\text{K}'$.

Refinement level	Mesh size	$\dim(\mathbb{V}_h(\Gamma))$	$\dim(\widetilde{\mathbb{V}}_h([\Gamma]))$
1	1.4142	13	6
2	0.70711	46	22
3	0.35355	178	87
4	0.17678	706	349
5	0.088388	2818	1401
6	0.044194	11266	5617

Table 2: Characteristics of the generalized mesh $\mathcal{M}_{\Gamma,h}^*$ and dimensions of boundary element spaces.

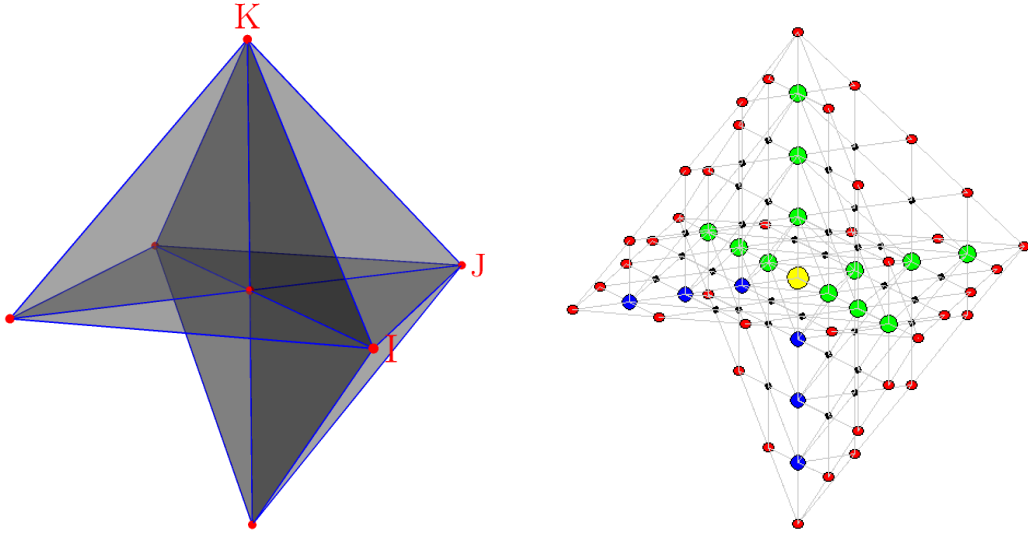


Figure 15: The mesh \mathcal{M}_Γ (left) and one of its refinements the mesh (right) where the vertices have been colored according to the number of generalized vertices attached to them. Red, black, blue, green and yellow stand for 1, 2, 3, 4, and 7, respectively.

With the intrinsic inflation algorithm, we construct the corresponding generalized mesh \mathcal{M}_Γ^* , and through mid point refinement, we construct a sequence of generalized meshes $\mathcal{M}_{\Gamma,h}^*$ with decreasing mesh sizes. In Table 2, we report the dimensions of the spaces $\mathbb{V}_h(\Gamma)$ and $\widetilde{\mathbb{V}}_h([\Gamma])$ depending on the level of refinement.

On this sequence of mesh, we assemble the matrices W and \widetilde{W} and report their condition number. For W , we use, as in [19], the “generalized condition number”, i.e. the ratio of the largest to the least *non-zero* singular values. We also report the dimension of the kernel of W – note that it corresponds exactly to $\dim(\mathbb{V}_h(\Gamma)) - \dim(\widetilde{\mathbb{V}}_h([\Gamma]))$, i.e. the dimension of the discrete single trace space $V_h([\Gamma])$. For the refinement level $l = 6$, the matrix W does not fit in memory.

Finally, we solve a the variational problem (37) with $\hat{g} = \pi_N(e_3)$, where $e_3 = (0, 0, 1)$, in two different ways. First, we solve the equation

$$Wx = L$$

Refinement level	cond(W)	dim(Ker(W))	cond(\widetilde{W})
1	1.9688	7	8.2226
2	4.3002	24	12.2002
3	6.7184	91	14.5876
4	9.988	357	16.2966
5	19.1046	1401	23.8994

Table 3: Condition numbers of the Galerkin BEM matrices.

Refinement level	n_1	n_2	e_1	e_2
1	3	6	2.473e-07	2.4728e-07
2	9	16	3.4876e-07	6.2505e-07
3	16	24	1.5859e-07	3.238e-07
4	19	27	1.2437e-07	1.3563e-07
5	24	32	6.9676e-08	1.0503e-07

Table 4: Resolution of the variational formulation, comparison between the quotient-space approach and the formulation without kernel.

where L is the vector of coefficients the linear form $\langle\langle \cdot, \dot{\mathbf{g}} \rangle\rangle$ in the multi-trace basis. We use the quotient-space iterative method, in this case, the conjugate gradient method (CG). We set the tolerance to 10^{-6} . Once the solution x is found, the function

$$\dot{u} := \sum_{\mathbf{v} \in \mathbf{S}_0(\mathcal{M}_{\Gamma, h}^*)} x_{\mathbf{v}} \omega_{\mathbf{v}}$$

is the approximate solution of the variational problem.

Second, we solve the equation

$$\widetilde{W}\tilde{x} = \tilde{L}$$

where $\tilde{L} = PL$, again using CG. The solution \tilde{x} is the vector of coefficients, in the basis of $\widetilde{V}_h(\Gamma)$, of the approximate solution \tilde{u} of (38).

We check that when \tilde{u} is a solution of (38), and if \dot{u} is chosen such that $[\dot{u}] = \tilde{u}$, then \dot{u} solves (37). Algebraically, one can find \dot{u} by applying the matrix P' to the coefficients of the solution \tilde{u} .

In Table 4, we report the numbers of iterations n_1 and n_2 observed in each case (respectively, for the resolution in the quotient space and with the modified matrix), and the residuals e_1 and e_2 defined by

$$e_1 := \|Wx - L\|_2, \quad e_2 := \|WP'\tilde{x} - L\|_2.$$

For both problems the tolerance of CG is set to $\varepsilon = 10^{-6}$.

Acknowledgement: The first author would like to thank Maxence Novel for his help in the proof of Theorem 2, and Nikolas Stott for his suggestions of presentation.

References

- [1] P. M. Adler, J.-F. Thovert, and V. V. Mourzenko. *Fractured porous media*. Oxford University Press, Oxford, 2013, pp. viii+175. ISBN: 978-0-19-966651-5.
- [2] C. Alboin et al. “Modeling fractures as interfaces for flow and transport in porous media”. In: *Fluid flow and transport in porous media: mathematical and numerical treatment (South Hadley, MA, 2001)*. Vol. 295. Contemp. Math. Pp. 13–24.
- [3] F. Alouges and M. Aussal. “FEM and BEM simulations with the Gypsilab framework”. In: *SMAI J. Comput. Math.* 4 (2018), pp. 297–318.
- [4] P. Angot, F. Boyer, and F. Hubert. “Asymptotic and numerical modelling of flows in fractured porous media”. In: *M2AN Math. Model. Numer. Anal.* 43.2 (2009), pp. 239–275.
- [5] D. N. Arnold, R. S. Falk, and R. Winther. “Finite element exterior calculus, homological techniques, and applications”. In: *Acta Numer.* 15 (2006), pp. 1–155.
- [6] M. Averseng. *Fracked meshes library*. <https://github.com/MartinAverseng/FracMeshLib>.
- [7] M. Averseng. “Weak representation of the Laplace hypersingular operator on a multi-screen”. In preparation. 2022.
- [8] M. Averseng, X. Claeys, and R. Hiptmair. “Approximation properties of finite elements on multi-screens”. In preparation. 2022.
- [9] J. Bannister, A. Gibbs, and D. P. Hewett. “Acoustic scattering by impedance screens/cracks with fractal boundary: Well-posedness analysis and boundary element approximation”. In: *Math. Models Methods Appl. Sci.* 32.2 (2022), pp. 291–319.
- [10] R. L. Berge, Ø. S. Klemetsdal, and K.-A. Lie. “Unstructured Voronoi grids conforming to lower dimensional objects”. In: *Comput. Geosci.* 23.1 (2019), pp. 169–188.
- [11] I. Berre, F. Doster, and E. Keilegavlen. “Flow in fractured porous media: a review of conceptual models and discretization approaches”. In: *Transp. Porous Media* 130.1 (2019), pp. 215–236.
- [12] I. Berre et al. “Verification benchmarks for single-phase flow in three-dimensional fractured porous media”. In: *Advances in Water Resources* 147 (2021), p. 103759.
- [13] J.-D. Boissonnat and M. Yvinec. *Algorithmic geometry*. Cambridge University Press, 1998.
- [14] J. L. Bryant. “Piecewise linear topology”. In: *Handbook of geometric topology*. North-Holland, Amsterdam, 2002, pp. 219–259.
- [15] A. Buffa and S. H. Christiansen. “The electric field integral equation on Lipschitz screens: definitions and numerical approximation”. In: *Numer. Math.* 94.2 (2003), pp. 229–267.
- [16] S. N. Chandler-Wilde et al. “Boundary element methods for acoustic scattering by fractal screens”. In: *Numer. Math.* 147.4 (2021), pp. 785–837.
- [17] P. G. Ciarlet. *The finite element method for elliptic problems*. Vol. 40. Classics in Applied Mathematics. Society for Industrial and Applied Mathematics (SIAM), Philadelphia, PA, 2002.
- [18] X. Claeys and R. Hiptmair. “Integral equations on multi-screens”. In: *Integral Equations Operator Theory* 77.2 (2013), pp. 167–197.

- [19] X. Claeys et al. “Quotient-space boundary element methods for scattering at complex screens”. In: *BIT* 61 (2021).
- [20] L. De Floriani and A. Hui. “Data Structures for Simplicial Complexes: An Analysis And A Comparison.” In: *Symposium on Geometry Processing*. 2005, pp. 119–128.
- [21] A. Ern and J.-L. Guermond. *Theory and practice of finite elements*. Vol. 159. Applied Mathematical Sciences. Springer-Verlag, New York, 2004.
- [22] C. Geuzaine and J.-F. Remacle. “Gmsh: A 3-D finite element mesh generator with built-in pre- and post-processing facilities”. In: *Internat. J. Numer. Methods Engrg.* 79.11 (2009), pp. 1309–1331.
- [23] R. Hiptmair and C. Urzúa-Torres. “Preconditioning the EFIE on screens”. In: *Math. Models Methods Appl. Sci.* 30.9 (2020), pp. 1705–1726.
- [24] E. Keilegavlen et al. “PorePy: an open-source software for simulation of multiphysics processes in fractured porous media”. In: *Comput. Geosci.* 25.1 (2021), pp. 243–265.
- [25] M. Kuna. *Finite elements in fracture mechanics*. Second Edition. Vol. 201. Solid Mechanics and its Applications. Theory—numerics—applications. Springer, Dordrecht, 2013.
- [26] J. M. Lee. *Introduction to topological manifolds*. Second. Vol. 202. Graduate Texts in Mathematics. Springer, New York, 2011.
- [27] A. Liu and B. Joe. “Quality local refinement of tetrahedral meshes based on 8-subtetrahedron subdivision”. In: *Math. Comp.* 65.215 (1996), pp. 1183–1200.
- [28] V. Martin, J. Jaffré, and J. E. Roberts. “Modeling fractures and barriers as interfaces for flow in porous media”. In: *SIAM J. Sci. Comput.* 26.5 (2005), pp. 1667–1691. ISSN: 1064-8275. DOI: 10.1137/S1064827503429363. URL: <https://doi.org/10.1137/S1064827503429363>.
- [29] E. Moise. *Geometric topology in dimensions 2 and 3*. Graduate Texts in Mathematics, Vol. 47. Springer-Verlag, New York-Heidelberg, 1977.
- [30] C. P. Rourke and B. J. Sanderson. *Introduction to piecewise-linear topology*. Springer Study Edition. Reprint. Springer-Verlag, Berlin-New York, 1982.
- [31] H. Whitney. *Geometric integration theory*. Princeton University Press, Princeton, N. J., 1957.

Index of notation

$\sigma_d(S)$	d -subsimplices of the simplex S	
$\mathcal{F}(S)$	facets of the simplex S	
$\sigma(S)$	subsimplices of the simplex S , including S	
$[S]$	convex hull of the simplex S	Eq. (1)
$[V_1, \dots, V_{n+1}]$	n -simplex oriented by the order (V_1, \dots, V_{n+1})	
$-[S]$	simplex S with the orientation opposite to $[S]$	
$[F]_{ [S]}$	facet F of S with the orientation induced by $[S]$	Eq. (2)
$\sigma_d(\mathcal{M})$	d -subsimplices of the triangulation \mathcal{M}	Eq. (5)
$\sigma(\mathcal{M})$	subsimplices of the triangulation \mathcal{M}	Eq. (5)
$\mathcal{F}(\mathcal{M})$	facets of the triangulation \mathcal{M}	Eq. (5)
$\overset{\leftarrow}{\underset{\mathcal{M}}{\longleftrightarrow}}$	adjacency in the triangulation \mathcal{M}	
$\text{st}(S, \mathcal{M})$	star of the subsimplex S of \mathcal{M}	Eq. (6)
$\text{lk}(S, \mathcal{M})$	link of the subsimplex S of \mathcal{M}	Eq. (7)
$\partial\mathcal{M}$	boundary of the triangulation \mathcal{M}	Eq. (8)
$ \mathcal{M} $	geometry of the mesh \mathcal{M}	Eq. (11)
$\mathcal{V}_{\mathcal{M}^*}, \mathcal{V}$	vertex set of \mathcal{M}^*	Definition 1
$\mathbf{K}_{\mathcal{M}^*}, \mathbf{K}$	set of elements of \mathcal{M}^*	Definition 1
$\mathcal{K}_{\mathcal{M}^*}, \mathcal{K}$	realization function of \mathcal{M}^*	Definition 1
$\mathcal{G}_{\mathcal{M}^*}, \mathcal{G}$	adjacency graph of \mathcal{M}^*	Definition 1
$\mathbb{F}(\mathcal{M}^*)$	split facets of \mathcal{M}^*	Eq. (12)
$\overset{F}{\underset{\mathcal{M}^*}{\longleftrightarrow}}, \overset{F}{\leftarrow}$	adjacency through F in \mathcal{M}^*	Eq.(13)
$\mathcal{N}_{\mathcal{M}^*}, \mathcal{N}$	neighbor function of \mathcal{M}^*	Eq. (14)
$\sigma_d(\mathcal{M}^*)$	subsimplices of \mathcal{M}^*	Definition 2
$[\mathbf{k}]_{\mathcal{M}^*}$	orientation of the simplex attached to \mathbf{k} assigned by the orientation of \mathcal{M}^*	Definition 5
$\text{st}(S, \mathcal{M}^*)$	generalized star of S in \mathcal{M}^*	Eq. (17)
$\mathcal{G}_{\mathcal{M}^*}(S), \mathcal{G}(S)$	graph between elements of $\text{st}(S, \mathcal{M}^*)$	Figure 5
$\mathbf{S}_d(\mathcal{M}^*)$	set of generalized d -subfacets of \mathcal{M}^*	Definition 6
$\mathbf{F}(\mathcal{M}^*)$	generalized facets, of \mathcal{M}^*	Eq. (19)
$\mathbf{F}_b(\mathcal{M}^*)$	boundary split facets of \mathcal{M}^*	Eq. (20)
$\partial\mathcal{M}^*$	boundary of \mathcal{M}^* , temporarily denoted by $\partial^*\mathcal{M}^*$	Definition 8
$\mathcal{M}_{\Omega \setminus \Gamma}^*$	fractured mesh	Section 4.1
$\mathcal{M}_{\Gamma}^*(\Omega)$	extrinsic inflation of \mathcal{M}_{Γ} via \mathcal{M}_{Ω}	Definition 11
$\Theta(T_1, T_2)$	geometric angle between T_1 and T_2	Eq. (23)
$\angle([T_1], T_2)$	oriented angle between $[T_1]$ and T_2	Eq. (24)
\mathcal{F}_{Γ}	set of all orientations of the facets of \mathcal{M}_{Γ}	Eq. (26)
\mathcal{M}_{Γ}^*	intrinsic inflation of \mathcal{M}_{Γ}	Definition 12
λ_V^K	barycentric coordinate	Eq.(30)
$\omega_{\mathbf{s}}$	Whitney form associated to the generalized d -subfacet \mathbf{s}	Definition 13
$\Lambda^d(\mathcal{M}^*)$	vector space of d -Whitney forms on \mathcal{M}^*	
Tr	trace operator for Whitney forms	Definition 14